Canadian Journal of
Fisheries and
Aquatic Sciences

Article

# Modeling coho salmon (*Oncorhynchus kisutch*) population response to streamflow and water temperature extremes

**J. Ryan Bellmore[a], Christopher J. Sergeant[b,c], Rebecca A. Bellmore[d], Jeffrey A. Falke[e], and Jason B. Fellman[f]**

[a]U.S. Department of Agriculture, Forest Service, Pacific Northwest Research Station, Juneau, AK, USA; [b]College of Fisheries and Ocean Sciences, University of Alaska Fairbanks, Juneau, AK, USA; [c]Flathead Lake Biological Station, University of Montana, Polson, MT, USA; [d]Southeast Alaska Watershed Coalition, Juneau, AK, USA; [e]U.S. Geological Survey, Alaska Cooperative Fish and Wildlife Research Unit, Fairbanks, AK, USA; [f]Alaska Coastal Rainforest Center and Environmental Science Program, University of Alaska Southeast, Juneau, AK, USA

Corresponding author: **Christopher J. Sergeant** (email: chris.sergeant@gmail.com)



## Abstract

Models that assess the vulnerability of freshwater species to shifting environmental conditions do not always account for short-duration extremes, which are increasingly common. Life cycle models for Pacific salmon (*Oncorhynchus* spp.) generally focus on average conditions that fish experience during each life stage, yet many floods, low flows, and elevated water temperatures only last days to weeks. We developed a process-based life cycle model that links coho salmon (*Oncorhynchus kisutch*) abundance to daily streamflow and thermal regimes to assess: (1) "How does salmon abundance respond to short-duration floods, low flows, and high temperatures in glacier-, snow-, and rain-fed streams?" and (2) "How does the temporal resolution of flow and temperature data influence these responses?". Our simulations indicate that short-duration extremes can reduce salmon abundance in some contexts. However, after daily flow and temperature data were aggregated into weekly and monthly averages, the impact of extreme events on populations declined. Our analysis demonstrates that novel modeling frameworks that capture daily variability in flow and temperature are needed to examine impacts of extreme events on Pacific salmon.

**Key words:** Life cycle, simulation modeling, pacific salmon, extreme events, thermal regime, flow regime

## Introduction

Scientists predict increasingly frequent bouts of intense air temperature and precipitation across the globe (Easterling et al. 2000). In rivers, these atmospheric changes can increase water temperature, flooding, and drought to thresholds that alter the population dynamics of aquatic species (Grimm and Fisher 1989; Omerod 2009; Milner et al. 2013; Ledger and Milner 2015). While these large-scale forces can change the mean and variability of environmental conditions across short (e.g., daily to weekly) to long (e.g., monthly to annual) time scales, modeling approaches designed to assess the vulnerability of aquatic species to shifting environmental conditions do not always account for short-duration extremes (Thornton et al. 2014). Many population models, for instance, run at timesteps (e.g., annual) that may be too coarse for examining events that are only a few weeks (e.g., extreme low flows) or a few days (e.g., flooding) in duration (see Adrian et al. 2012; Nadeau et al. 2017). As the frequency and severity of extreme events increase, novel modeling frameworks that capture daily to weekly variability in environmental conditions are needed to examine impacts to aquatic species.

In the watersheds of the Northeast Pacific Coastal Temperate Rainforest—which extends from southern Alaska to northern California, USA—climate change is altering patterns of streamflow and water temperature via elevated air temperature, increased frequency and intensity of rainfall, and accelerated glacier retreat (reviewed in Bidlack et al. 2021). There is a continued need to assess the vulnerability of Pacific salmon (*Oncorhynchus* spp.) to these changes because they are a culturally and economically valuable group of species in the region (Augerot and Foley 2005; Schindler et al. 2010; Johnson et al. 2019). A growing body of literature has been dedicated to determining how growth and survival of different salmon life stages (eggs, juveniles, adult spawners) will respond to shifting environmental conditions (Crozier et al. 2008; Zhang et al. 2019), but few studies have examined the cumulative impacts of short-duration extreme events such as flooding and drought across multiple freshwater life stages.

Climate change projections predict increased frequency of autumn and winter storms and more intense summer drought and higher air temperatures for coastal watersheds along the northern portion of the Northeast Pacific Coastal Temperate Rainforest. For example, in southeastern Alaska, up to 97% of extreme precipitation events arise from atmospheric rivers—heavy rain caused by moisture originating in the tropics—and occur primarily from August through November (Sharma and Déry 2020). These intense rains of-

ten create large flood events when salmon eggs are in the gravel and increase the probability of embryo mortality due to streambed scour (Sloat et al. 2017). The magnitude of these floods can be amplified when heavy rains fall on top of existing snowpack (rain-on-snow floods; McCabe et al. 2007). Furthermore, the frequency of autumnal atmospheric rivers is expected to increase through the remainder of this century (Radić et al. 2015), with unknown implications for freshwater habitat quality and quantity for Pacific salmon.

Summer drought caused by warming air temperature and reduced snowpack (Walsh et al. 2017; Littell et al. 2018) can directly affect the physiology of salmon by increasing water temperature, reducing habitat availability, slowing or blocking the upstream migration of spawners (Bowerman et al. 2018), and creating more frequent periods of low dissolved oxygen (Sergeant et al. 2017). Even in a typically wet landscape such as Prince William Sound (Cordova, Alaska annual average rainfall = 234 cm; Western Regional Climate Center, https://wrcc.dri.edu/), an extreme heat wave in 2019 led to streambed drying that blocked the upstream migration of spawning salmon across multiple watersheds (von Biela et al. 2022). Indeed, the impacts of drought to salmon spawning in the rainforest watersheds of coastal Alaska have been locally documented for decades (Murphy 1985). Summer water temperatures in nonglacierized, low gradient watersheds are especially sensitive to changes in air temperature, and maximum observed water temperature tends to increase with greater lake and wetland coverage (Mauger et al. 2017; Winfree et al. 2018). Therefore, coastal Alaska watersheds are projected to warm due to increasing air temperatures and reduced glacier and snowmelt contributions to surface waters (Shaftel et al. 2020).

In southern coastal Alaska, streams fed by glaciers, snow, and rain create a complex array of streamflow and thermal regimes that may differentially affect the growth and survival responses of salmon populations to extreme events (Winfree et al. 2018; Sergeant et al. 2020). The current and future impacts of these climate-induced changes to salmon in coastal Alaskan rivers are an ongoing field of investigation (Leppi et al. 2014; Cunningham et al. 2018; Jones et al. 2020). Most of this work has involved fitting models to salmon abundance data from various life stages and mean environmental conditions (e.g., mean monthly discharge or mean weekly water temperature). Existing tools such as the Shiraz life cycle model (Scheuerell et al. 2006) are powerful and widely used for the conservation and management of salmon populations, but present three research hurdles: (1) models often require detailed empirical data on population productivity or habitat carrying capacity across different life stages, (2) environmental conditions during extreme events may lie outside the bounds of existing statistical relationships used in these models, and (3) data are often coarsely aggregated across months or life stages. At the remote northern edge of the range of Pacific salmon, where populations are most abundant (Augerot and Foley 2005), watershed- to reach-scale habitat data are often sparse or absent. Also, extreme events tend to occur at daily to weekly time steps; therefore, life cycle models that aggregate streamflow and water temperature values across weeks, months, or life stages may not characterize the importance of short-term extreme events to which individual salmon respond and which may ultimately affect population productivity.

To examine how short-duration extreme events impact salmon populations in coastal Alaska watersheds, we developed a process-based life cycle model that mechanistically links salmon success at each life stage to daily streamflow and thermal regimes. We provide examples of model behavior using coho salmon (*Oncorhynchus kisutch*) from three divergent watershed types in southeastern Alaska. We chose coho salmon because they tend to spend the longest period in freshwater relative to other anadromous and semelparous species within the genera *Oncorhynchus* (Quinn 2018) and are an important subsistence-, commercial-, and sport-harvested salmon species found in Gulf of Alaska watersheds. The model examines two primary questions: (1) "How does salmon abundance respond to short-duration floods, low flows, and high water temperatures in glacier-, snow-, and rain-fed streams?" and (2) "How does the temporal resolution of streamflow and water temperature data influence modeled coho salmon abundance?". To explore the first question, we varied the magnitude of winter floods, summer low flows, and summer water temperature and assessed the sensitivity of salmon populations to shifting environmental conditions. To explore the second question, we aggregated daily flow and temperature data at weekly and monthly time intervals to assess how the temporal resolution of data influenced modeled salmon abundance. Since the glacier-, snow-, and rain-fed stream analyses are based on one year of empirical discharge and water temperature, we also evaluated model response to interannual hydrologic variability using a 23-year time series from Staney Creek, a rain-fed system in southeastern Alaska. Our analysis illustrates that short-duration extreme events can strongly affect salmon populations, and highlights the need for process-based models that operate at finer temporal resolution (e.g., daily).

## Methods

### Salmon life cycle model description

We constructed a *system dynamics* model that mechanistically links salmon survival at each freshwater life stage to daily thermal and streamflow regimes (Poff et al. 1997; Caissie 2006). In general, regimes refer to distributions of values across multiple temporal and spatial scales; for this study, we specifically assess variation of streamflow and water temperature at the daily time scale. The system dynamics modeling approach focuses on causal linkages and feedback loops that drive nonlinear dynamics in complex systems (Ford 2009). Our model tracks cohorts of salmon through four life stages: spawning adults, incubating eggs, freshwater juveniles, and smolts/marine adults (Fig. 1). The structure of the model includes four primary feedback loops that regulate the dynamics of the population through time (Fig. 1). There is one reinforcing or positive feedback loop (population growth) that grows the salmon population and three density-dependent balancing, or negative, feedback loops that constrain popu-

**Fig. 1.** Coho salmon life cycle model. Illustration by Cecil Howell. Positive interactions indicate that the two components change in the same direction, while negative interactions indicate that the two components change in opposite directions. For example, more spawners equate to higher spawner density (positive interaction), but higher spawner density equates to lower dissolved oxygen (negative interaction), and lower dissolved oxygen equates to higher pre-spawn mortality (also a negative interaction).

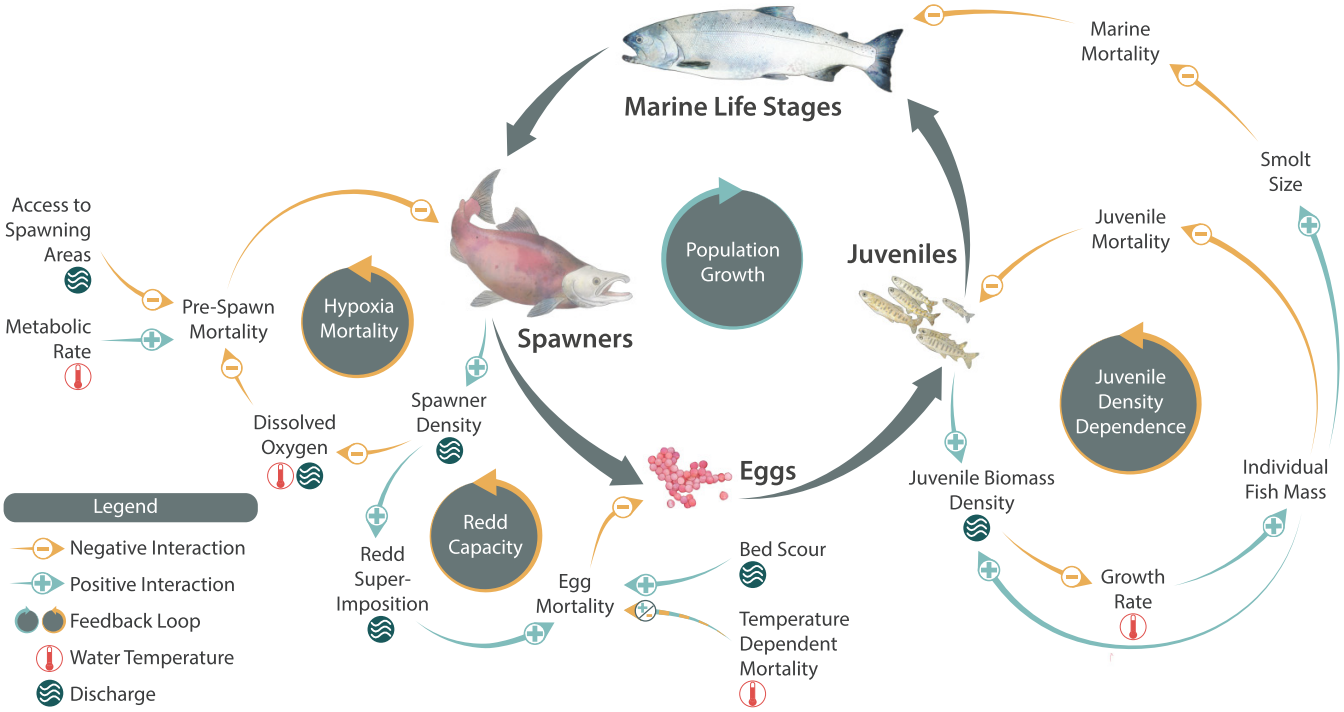




lation growth, which include: juvenile density dependence, redd carrying capacity, and pre-spawn hypoxia mortality. The strength of these balancing feedbacks is influenced by the size of the salmon population, as well as freshwater streamflow and (or) thermal regimes. For instance, greater juvenile salmon density increases competition for space and food, which reduces juvenile growth and survival. The strength of this negative feedback is influenced by changes in wetted area (streamflow) that reduce or increase fish density, and water temperatures that mediate bioenergetic demand for limited food resources. Streamflow and thermal regimes also have numerous density-independent effects on salmon productivity in the model (Fig. 1); e.g., high streamflow can increase egg mortality by scouring salmon redds (Montgomery et al. 1996).

The model was developed to explore flow and temperature effects at the spatial scale of geomorphic segments (~100 m—10 km), within which flow, temperature, and geomorphic conditions were assumed to be homogenous (*sensu*Scheuerell et al. 2006). However, in locations where spatially explicit daily flow and water temperature are available, this approach could be scaled to entire watersheds (e.g., Jorgensen et al. 2021). The model was constructed in the system dynamics software, Stella Architect version 2.0 (ISEE Systems, Lebanon, NH, USA). All model simulations were run on a daily time step using the Euler integration method. While we chose coho salmon for this initial application, the model could be adapted for other Pacific salmon species that spawn and rear in lotic environments. In the sections below, we provide a detailed description of the processes that influence salmon survival during each life stage. Parameter values are provided in Table S1.

## Adult spawning salmon

In the model, adult coho salmon enter streams to spawn on 1 October if river discharge is sufficient to provide a depth of 18 cm at the stream mouth (Bjornn and Reiser 1991). If streamflow is too low for salmon entry, fish stage at the river mouth until discharge increases, during which time we assume a constant rate of staging mortality ($StagingMort = 0.01/day$). Spawning commences 14 days after freshwater entry, which is appropriate in the small Southeast Alaska watersheds evaluated in this paper, where migration distance to spawning areas is short (<5 km), and similar to other streams in British Columbia and Alaska (English et al. 1992; Hetrick and Nemeth 2003). Prior to spawning, streamflow and temperature influence pre-spawn mortality via both density-independent and density-dependent processes. Density independent pre-spawn mortality is a function of spawner condition factor at each time step ($CF_{spawner,t}$):

$$(1)\quad PrespawnMort_t = 1 - \frac{CF_{spawner,t}{}^{\beta_{spawner}}}{CF_{spawner,t}{}^{\beta_{spawner}} + HS_{spawner}{}^{\beta_{spawner}}}$$

where $HS_{spawner}$ is the value of $CF_{spawner}$ at which daily spawner survival is 50% per day, and $\beta_{spawner}$ is a shape parameter that influences the slope of the sigmoidal relationship (Fig. S1). Because adult Pacific salmon generally do not feed after they enter freshwater, fish mass ($Mass_{spawner}$) and condition factor decline daily due to fish respiration:

$$(2) \quad CF_{spawner,t} = \frac{Mass_{spawner,t} - \left(Mass_{spawner,t} \times resp_{spawner,t}\right)}{InitialMass_{spawner}}$$

where $InitialMass_{spawner}$ is the average weight of spawners on the first day of freshwater entry and $resp_{spawner}$ is the daily mass-specific rate of spawner respiration. Water temperature influences this process by mediating respiration rates, which were calculated using published bioenergetic equations for coho salmon (Hanson et al. 1997; Deslauriers et al. 2017). As water temperatures rise, respiration increases and spawner mass declines, which increases prespawn mortality.

Salmon oxygen demand increases with water temperature and when low streamflow increases salmon density per area. If oxygen demand exceeds the rate of reaeration with the atmosphere, dissolved oxygen concentrations can become hypoxic and reach lethal thresholds that cause density-dependent mortality (Sergeant et al. 2017). We assume that the spawning population dies at a constant proportion of 0.5 (*HypoxiaMort*) every day that instantaneous dissolved oxygen concentrations dip below a critical threshold ($[O_2]_{threshold}$), which we assumed to be 3.5 mg $O_2$ $L^{-1}$ (approximated based on Washington State Department of Ecology 2002). This mortality rate allows oxygen concentrations to recover without depleting our entire population in one day. While we do not know of any published functional relationships relating daily spawning salmon mortality to dissolved oxygen concentrations, the 0.5 proportion is realistic and possibly conservative in comparison to other studies of premature mortality in response to hypoxia (Tillotson and Quinn 2017). We used a simplified representation of the dynamic dissolved oxygen equations from Sergeant et al. (2017) to calculate the influence of spawning salmon on dissolved oxygen:

$$(3) \quad [O_2] = [O_2]_{saturation} + \left(k_{(T^\circ C)} - O_{2_{resp}}\right)$$

where $[O_2]_{saturation}$ is the dissolved oxygen saturation concentration at atmospheric equilibrium, $K_{(T^\circ C)}$ is the hourly rate of oxygen reaeration at ambient water temperature ($T$), and $O_{2_{resp}}$ is the rate (1/hour) of oxygen respiration due to spawning salmon. The concentration of dissolved oxygen at complete saturation varies with water temperature and was calculated following Benson and Krause (1980). The reaeration rate at ambient water temperature ($T$) is calculated following Elmore and West (1961):

$$(4) \quad k_{(T^\circ C)} = k_{(20^\circ C)} * 1.024^{(T-20)}$$

where $k_{(20^\circ C)}$ is the oxygen reaeration rate when water temperature is 20°C and was calculated based on average water depth (m) and velocity (m/s) using the energy dissipation model (Owens et al. 1964). Salmon respiration was calculated using a bioenergetics model (Trudel et al. 2004; Holtgrieve and Schindler 2011) that relates oxygen consumption to individual salmon mass ($W$; g), swim speed ($U$; cm/s), and water temperature ($T$; °C) as:

$$(5) \quad O_{2_{resp}} = N_{salmon}\left(\chi Mass_{spawner,t}{}^{\tau} * e^{\varphi T} * e^{\nu U}\right)$$

Where $N_{salmon}$ is the number of spawning salmon per liter of water ($salmon/L = salmon/m^2 \times 1/depth\ (m) \times m^3/1000\ L$), $\chi$ is the standard metabolic rate of 1 g fish at 0°C, and $\tau$, $\varphi$, and $\nu$ are coefficients describing the metabolic costs of mass, temperature (T), and swim speed ($U$), respectively.

## Eggs

For salmon that survive pre-spawn mortality, the proportion of eggs that are successfully deposited is influenced by the redd carrying capacity of the reach (i.e., amount of suitable spawning gravels). This density-dependent feedback is caused by salmon superimposing their redds on top of other redds as salmon densities increase and (or) the amount of suitable spawning habitat decreases, such as when streamflow is low (Maunder 1997). The number of eggs that are successfully deposited and not excavated by superimposition ($Egg_{success}$) is given by the function (Maunder 1997):

$$(6) \quad Egg_{success} = (K_{redd} * Fecundity) \cdot \left(1 - \exp\left(-\frac{N_{spawners} * P_{female}}{K_{redd}}\right)\right)$$

where $K_{redd}$ is redd carrying capacity, *Fecundity* is the average number of eggs a female deposits, $N_{spawners}$ is the number of spawners, and $P_{female}$ is the proportion of spawners that are female. $K_{redd}$ was calculated by multiplying stream wetted area by the proportion of habitat that is suitable for spawning ($P_{suitable}$) and dividing by the average area of an individual redd ($A_{redd}$). This formulation assumes that the probability of salmon spawning is equal across all suitable spawning habitat.

For eggs that are successfully deposited, the rate of egg incubation and alevin development is a function of water temperature. In warmer waters, fewer days are required for egg hatch and fry emergence. The number of days from egg deposition to fry emergence was calculated using species-specific temperature-embryo development relationships (Beacham and Murray 1990). The model tracks the cumulative number of days since egg deposition, and the average water temperature during the incubation period. Fry emergence occurs when the cumulative number of days exceeds the number of days necessary for emergence at a given temperature (Beacham and Murray 1990). During this period, eggs and alevins are susceptible to two forms of mortality: (1) temperature-dependent mortality primarily associated with high (>15°C) and low (<1°C) water temperatures, and (2) scouring of egg pockets during high streamflow that mobilizes the stream bed. Daily mortality rate at a given water temperature was calculated by converting total life stage mortality from Beacham and Murray (1990) into daily temperature-dependent mortality rates that varied from day-to-day with

fluctuating water temperatures. Daily mortality was selected based on a graphical relationship between water temperature and daily mortality (Fig. S2) and then multiplied by a correction factor of 1, which adjusted temperature-dependent mortality in our sensitivity and uncertainty analyses (see the *Model validation and sensitivity analysis* section). Streamflow-induced egg mortality was calculated as the proportion of the stream bed where scour depth exceeds egg burial depth ($d_{egg}$; cm), following Goode et al. (2013):

$$(7) \quad P\left(\geq \mathrm{d}_{egg}\right) = e^{-d_{egg}\left(\varepsilon e^{-1.52\tau^*/\tau_c^*}\right)}$$

where $\tau^*$ is Shields stress on the stream bed and $\tau_c^*$ is the critical Shields stress that would mobilize the median stream bed grain size predicted as an empirical function of channel slope ($\tau_c^* = 0.15 \times Slope^{0.25}$; Lamb et al. 2008). The coefficient $\varepsilon$ determines the strength of egg pocket scour. Shields stress $\tau^*$ on the stream bed is calculated from channel slope ($S$), average water depth ($z$; which varies with daily discharge), and median sediment size ($D_{50}$):

$$(8) \quad \tau^* = \frac{pgzS}{(p_s - p)\,gD_{50}}$$

where $p_s$ and $p$ are substrate (2.65 kg/m$^3$) and water density (1 kg/m$^3$), and $g$ is acceleration due to gravity (Gordon et al. 2004).

## Freshwater juveniles

Surviving eggs and alevins emerge as free-living juvenile salmon. In the juvenile life stage, fish growth is modeled using bioenergetics equations that link fish size to temperature and streamflow. Once fry emerge and begin feeding, their wet mass (g) at time $t$ is a function of food consumption and energy demands:

$$(9) \quad JuvenileMass_t = JuvenileMass_{t-1} + (Cons_t \times AE) - Resp_{juvenile,t}$$

where $Cons_t$ is the rate of food consumption (g g$^{-1}$ day$^{-1}$), $AE$ is the amount of consumed food that is assimilated, and $Resp_{juvenile,t}$ is the rate of juvenile respiration. $Resp_{juvenile,t}$ is a function of water temperature, fish mass, and activity costs calculated from published fish bioenergetics model equations (Hanson et al. 1997; Deslauriers et al. 2017) and parameterized with values for coho salmon. $Cons_t$ is a function of water temperature, food availability, and fish density:

$$(10) \quad Cons_t = JuvenileMass_{t-1} \times Cons_{max} \times f_1(Temp) \times f_2(PreyAvailability, DensityDep)$$

where $Cons_{max}$ is the size-specific maximum rate of prey consumption when temperature conditions are optimum; and $f_1$ and $f_2$ are functions that range from 0 to 1 and describe the limiting effects of water temperature ($f_1$), and prey availability and density-dependence ($f_2$) on consumption. Existing bioenergetics equations parameterized with values for coho salmon were used to calculate $Cons_{max}$ and the limiting effects of temperature on consumption $f_1$ (*Temp*) (Hanson et al. 1997; Deslauriers et al. 2017). The limiting effect of prey availability and juvenile density-dependence ($f_2$) is described by a type II functional response:

$$(11) \quad f_2 = \frac{PreyBiomass}{PreyBiomass + \left(HS_{Prey} + \gamma_y \times FishBiomassDensity\right)}$$

where *PreyBiomass* is the amount of prey (e.g., aquatic and terrestrial insects or fish eggs) assumed to be available to juvenile fish per unit of wetted area (g/m$^2$), $HS_{prey}$ is the density-independent prey biomass half-saturation level, and $\gamma_Y$ is a dimensionless density-dependence parameter that adjusts consumption rates for juvenile salmon biomass density (*FishBiomassDensity*; g/m$^2$). Juvenile biomass density varies with streamflow and was calculated by multiplying individual fish mass by the number of fish and dividing by stream wetted area at time $t$.

Fish growth affects both density-dependent *starvation* and *size-based* mortality. Starvation mortality ($Starve_{mort}$) occurs when metabolic costs (respiration) exceed energy intake via consumption, which causes fish to lose mass. Streamflow affects starvation mortality by mediating fish densities and foraging success (see eq. 12), while water temperature mediates consumption and respiration rates. We used juvenile condition factor ($CF_{juv}$) to estimate daily starvation mortality at time $t$ following Railsback et al. (2009), which assumes that as $CF_{juv}$ decreases with weight loss, more juvenile fish succumb to starvation:

$$(12) \quad Starve_{mort} = \alpha_{starve}\left(1 - \frac{CF_{juv,t}{}^{\beta_{starve}}}{CF_{juv,t}{}^{\beta_{starve}} - HS_{starve}{}^{\beta_{starve}}}\right)$$

where $HS_{starve}$ is the value of $CF_{juv,t}$ at which daily juvenile survival is 50% per day, $\beta_{starve}$ is a shape parameter that influences the slope of the sigmoidal relationship, and $\alpha_{starve}$ is a coefficient that describes the strength of the function (Fig. S3). Condition factor was calculated at each time step by dividing fish mass by the "healthy" mass for a fish at its length (Railsback et al. 2009), as follows:

$$(13) \quad CF_{juv,t} = \frac{JuvenileMass_t}{\alpha_{growth} \times Length_t{}^{\beta_{growth}}}$$

where $\alpha_{growth}$ and $\beta_{growth}$ describe the relationship between fish mass and fork length. When $CF_{juv}$ is less than one, it indicates that fish have lost mass due to starvation and have fallen below the mass of a "healthy" fish at its length. Fish length is calculated as:

$$(14) \quad Length_t = \left(\frac{JuvenileMass_t}{\alpha_{growth}}\right)^{1/\beta_{growth}}$$

When fish mass decreases during starvation, we assume $Length_t$ (mm) remains the same, and fish only resume growing in length once $CF_{juv}$ returns to 1.

Size-based mortality ($Size_{mort}$) assumes that $Length_t$ influences susceptibility to mortality from a variety of sources (e.g., predation, scouring streamflow, and disease). Following

Railsback et al. (2009) and Benjamin et al. (2020), we model mortality as an exponentially decreasing function of length:

$$(15)\quad Size_{mort} = \alpha_{size} \times e^{(\beta_{size} L_t)}$$

where $\alpha_{size}$ and $\beta_{size}$ are parameters that describe the strength and the shape of the function. Size-based mortality is a density-dependent process in the model because fish size is influenced by juvenile density (eq. 11).

## Marine adults

After fry spend approximately one year in the stream, juvenile fish undergo smoltification and begin their migration downstream to the ocean on 1 May. Mortality during the marine life stage is a function of the length of smolts ($Length_{smolt}$) when they leave freshwater:

$$(16)\quad MarineMortality = 1 - \left( \frac{Survival_{max} \times Length_{smolt}{}^{\beta_{smolt}}}{Length_{smolt}{}^{\beta_{smolt}} + HS_{smolt}{}^{\beta_{smolt}}} \right)$$

where $Survival_{max}$ is the maximum proportion of fish that survive in the ocean, $HS_{smolt}$ is the value of $Length_{smolt}$ at which marine survival is 50% of $Survival_{max}$, and $\beta_{smolt}$ is a shape parameter that influences the slope of the relationship. $Length_{smolt}$ is equal to the maximum size that juveniles attain in freshwater before they begin migrating downstream on 1 May. Marine mortality is a density-dependent process. Greater modeled fish densities during the juvenile life stage can result in smaller smolts that have lower ocean survival. This equation was parameterized to fit an observed relationship between smolt size and adult returns at a permanent weir in Auke Creek in Juneau, Alaska (Lum 2003), which is the best available long-term data set near our modeled streams (Fig. S4).

## Model parameterization

We parameterized the model with one year of average daily streamflow and temperature data from moderately glacier-fed (Cowee Creek), snow-fed (Fish Creek), and rain-fed (Peterson Creek) streams in proximity to Juneau, Alaska (Fig. 2). These three streams were selected because they had year-round paired daily water temperature and discharge measurements, were near one another (maximum distance between two streams approximately 40 km), and were, therefore, subject to similar large-scale climate patterns. Despite experiencing similar weather conditions, the hydrographs, thermal profiles, and watershed characteristics of these streams are distinctly different from one another and reflect the diversity existing across thousands of glacier-, snow-, and rain-fed rivers draining into the Gulf of Alaska and further south throughout the Pacific coastal temperate rainforest (Table 1, Fig. 2; O'Neel et al. 2015; Winfree et al. 2018; Sergeant et al. 2020). With 11% snow and ice coverage within its watershed, Cowee Creek receives higher runoff in the summer with cooler year-round water temperature relative to our two other modeled streams. In contrast to larger glacier-fed systems with greater ice coverage (e.g., >20%), Cowee Creek represents smaller glacial watersheds in southern coastal Alaska and northern BC that are transitioning from ice-snow-fed streamflow patterns to snow-rain-fed as headwater glaciers recede. For brevity, we refer to Cowee Creek as a "glacier" stream in this study. Fish Creek is characteristic of snowmelt watersheds, with higher snow-fed streamflow in the spring and early summer (May–July) that moderate water temperatures and typically sustain streamflow during drought periods. Rain-fed Peterson Creek has more stochastic streamflow patterns with higher high-flows, and lower low-flows relative to baseflow, as well as warmer summer water temperatures than the other streams. Like other low-elevation watersheds in the region classified as rain-fed, Peterson Creek is also influenced by snowmelt runoff that is generally limited to the spring and does not greatly influence summer discharge.

We normalized streamflow data and homogenized channel morphology across our three modeled streams to remove the influence of watershed size on flow magnitude and to isolate differences in streamflow and thermal patterns in glacier-, snow-, and rain-fed streams that salmon populations experience. For each stream, the proportion of annual discharge occurring on a given day was divided by the average of the annual discharge across all three streams. This procedure retained differences in streamflow seasonality amongst the stream types, while keeping the total annual discharge the same. Streamflow values were converted to average wetted width and water depth ($z$) using graphic relationships between total discharge and width/depth (Fig. S5), and water velocity was solved for using the continuity equation (Gordon et al. 2004). We used the same graphical relationships between discharge and width/depth in each stream type, which were constructed by averaging channel morphology information (bankfull width, bankfull depth, channel gradient, bank angles) collected near discharge monitoring stations in each watershed. We also assumed channel gradient was the same in the three streams (0.022 m/m). Although glacier-, snow-, and rain-fed streams can have different channel morphology and hydraulics, we kept them the same to examine generalizable differences between stream types (as described above). Pebble count surveys (Wolman 1954) were conducted in each stream near the locations where streamflow and temperature data were collected and were used to calculate an average median grain size ($D_{50}$) across sites used in model runs (3 cm).

We also parameterized the model with a 23 year time-series (1997–2019) of temperature and streamflow data from Staney Creek, a rain-fed stream located on Prince of Wales Island, Alaska. In contrast to the generalized stream types described above, where simulations were based on one year of flow and temperature data, long-term data from Staney Creek allowed us to explore how natural observed fluctuations in discharge and water temperature influenced population abundance over time. Discharge to width-depth relationships (Fig. S5), channel gradient (0.020 m/m), and $D_{50}$ (5 cm) for Staney Creek were estimated from the NetMap synthetic stream network for the Tongass National Forest (Benda et al. 2007, 2016).

For all scenarios we used the same global set of model parameter values for the exponents, coefficients, and other parameters in the model equations (Table S1). When available,

**Fig. 2.** Daily, weekly, and monthly aggregated flow and thermal regime data for representative stream runoff types. See the Methods subsection, *Model parameterization*, for a description of how discharge data were normalized to reduce the influence of watershed size on flow magnitude across the three modeled streams.

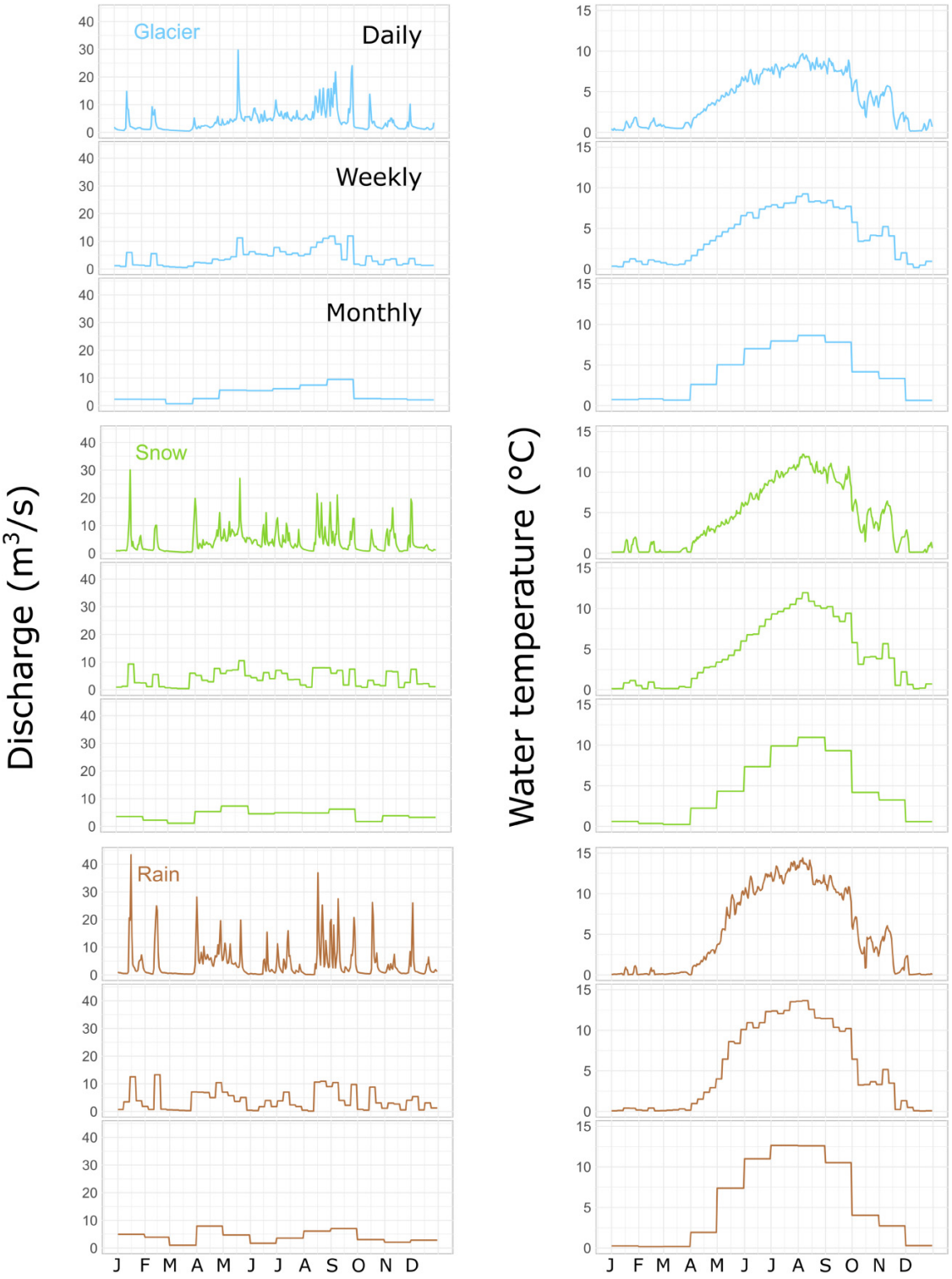


we used published or derived values from published studies. In cases where no literature values existed, we adjusted parameter values to produce model runs that were stable (i.e., populations maintained a value above zero) and that produced reasonable estimates of fish abundance. To examine how the value of these assumed variables influenced modeled outcomes, we included 11 of these parameters in model sensitivity and uncertainty analyses (described below).

**Table 1.** Watershed landcover, elevation, and precipitation characteristics used to create generalized glacier-, snow-, and rain-fed streams. Mean annual precipitation is averaged across the years 1981–2010.

| | Cowee | Fish | Peterson | Staney | Data source |
|---|---|---|---|---|---|
| Primary runoff source | Glacier | Snow | Rain | Rain | Sergeant et al. 2020 |
| Ice coverage (%) | 11% | 0% | 0% | 0% | Sayre et al. 2020 |
| Forest coverage (%) | 61% | 73% | 95% | 87% | Sayre et al. 2020 |
| Wetland coverage (%) | 16% | 25% | 5% | 13% | Sayre et al. 2020 |
| Watershed area ($km^2$) | 118 | 36 | 44 | 159 | Biles 2019 |
| Mean watershed elevation (m) | 603 | 474 | 231 | 230 | Biles 2016 |
| Maximum watershed elevation (m) | 1717 | 956 | 548 | 839 | Biles 2016 |
| Mean annual precipitation (mm) | 1577 | 1734 | 1570 | 2290 | http://www.climatewna.com/ |



## Model validation and sensitivity analysis

To explore model validity, we assessed whether initializing the model across a range of parent spawner abundance values produced a realistic number of adult spawning offspring (spawner-to-spawner relationship) that mimics density-dependent patterns observed in natural salmon populations. For each stream type (glacier, snow, and rain), we varied the number of parent spawners from 2 to 200 at model initialization and then plotted the number of parent spawners against the number of adult spawning offspring produced after one generation (4 years). We also ran the model for 40 years (10 generations) using the same empirical time series of water temperature and streamflow across all years to examine if equilibrium salmon densities produced by the baseline habitat characteristics in the model were realistic for watersheds in the region.

We conducted a global sensitivity analysis to examine how uncertainty in the value of model parameters influenced modeled outcomes, and to identify the importance of each parameter in model simulations. In global sensitivity analyses, the values of uncertain parameters are adjusted simultaneously. Eleven model parameters were selected for this analysis that were distributed across all life stages and processes that control fish mortality (Table S1). Selected parameters were generally those with less certainty (i.e., assumed or calculated values). The range of "uncertainty bounds" surrounding the value of each parameter were adjusted to account for perceived uncertainty in the value of the parameter: ±10% for literature-derived values, and ± 25% for parameter values that were assumed (Table S1). Sensitivity analyses were then conducted using a Latin hypercube sampling design (McKay et al. 1979) that ensures adequate sampling across the entire range of each parameter.

We conducted a 1000-simulation global sensitivity analysis to produce 1000 separate estimates of returning salmon spawners. All simulations were initialized with 100 spawners and run for 32 years (11 680 days). Using the matrix of input and output parameter values across the 1000 simulations, we conducted a random forest analysis to calculate the importance for each parameter, including interactions with all other parameters in determining spawner returns (Random Forest 4.6–2; Liaw and Wiener 2002; R Core Team 2019). Importance values represent the change in prediction error of the regression tree when the value of a given parameter is changed while values for all other parameters remain the same (Harper et al. 2011). Importance values for each parameter were normalized by the sum of importance values for all parameters.

## Streamflow and thermal regime scenarios

We examined the sensitivity of coho salmon populations to increasing intensities of winter floods, summer droughts, and summer heat in modeled glacier-, snow-, and rain-fed streams. We created four separate winter flood scenarios from the baseline flow data for each modeled stream by increasing the empirical discharge observed on each day from January 13–19 by increments of 25%, 50%, 75%, or 100%. This 7 day time period encompasses the dates of empirical maximum daily winter flows across all three modeled streams. Winter floods are expected to increase in magnitude in southern coastal Alaska as the elevation of the rain-snow transition zone within watersheds increases due to warmer air temperature, thereby creating more immediate runoff due to rain and resulting in greater hydrograph flashiness (Shanley et al. 2015; Beamer et al. 2017). While a 100% winter flood increase may not be realistic in some contemporary watersheds, we justify this scenario for two reasons: (1) it acts as a threshold that provides insight into how dramatic hydrologic shifts impact salmon populations and (2) it is actually a realistic scenario for some watersheds. For example, in Fish Creek, used here as the model snow-fed stream, maximum instantaneous discharge across the official period of record has been recorded as high as 82 $m^3\ s^{-1}$ (https://waterdata.usgs.gov/nwis/inventory?agency_code=USGS&site_no=15109000), which is approximately 260% higher than the maximum daily normalized flow on which winter flood scenarios are based (the non-normalized empirical maximum daily discharge in our Fish Creek time series was 17.4 $m^3\ s^{-1}$).

To create four summer drought scenarios from the baseline flow data for each modeled stream, we decreased the daily discharge for a two-week period during the summer (29 July–13 August) by increments of 25%, 50%, 75%, or 100% less than the lowest empirical discharge observed during that period. For example, the lowest discharge observed in the rain-fed stream between July 29-August 13 was 0.104 $m^3\ s^{-1}$; therefore, in the 25% decrease scenario, each day was set to 0.078 $m^3\ s^{-1}$. This time period encompassed the summertime

minimum flows for the rain- and snow-fed streams, and was near the minimum for the glacier-fed stream. For the 100% decrease in streamflow scenario (i.e., stream drying), we assumed that the wetted length of the channel decreased by 50% (from 1 to 0.5 km) to represent a situation where wetted habitats (i.e., isolated pools) are only present in half of the reach. Stream drying remains relatively rare in southern coastal Alaska, but during a July 2019 heat wave, numerous rain-fed streams surrounding Juneau, Alaska, were completely dry or only contained isolated pools (unpublished observations by RAB and JRB). Additionally, during the latter 2 weeks of August 2019, the discharge of a gaged rain-fed creek in Cordova, Alaska, only ranged from 0.02 to 0.08 $m^3 s^{-1}$ and was representative of many other rain-fed watersheds in Prince William Sound (von Biela et al. 2022).

To create four summer heat scenarios from the baseline water temperature data for each modeled stream, we increased the highest daily maximum water temperature during the same two-week drought period by 10%, 20%, 30%, and 40%. Since low streamflow is typically associated with increased water temperature, we also created four scenarios combining the concurrent adjustments of summer drought and summer heat (for example, 25% decrease in lowest minimum streamflow and 10% increase in peak water temperature). Finally, we created a single scenario combining the most extreme streamflow and thermal regime shifts (100% increase in winter maximum flood magnitude, 100% decrease in summer minimum streamflow magnitude, and 40% increase in peak summer water temperature). We acknowledge that some of these scenarios are unlikely (e.g., we would not expect streams with glacier influence to dry up in the summer), but nevertheless, within the context of a sensitivity analysis they allowed us to examine the relative sensitivity of these stream types to changes in streamflow and temperature.

All simulations were conducted for one km of stream, and we assumed that 50% of the stream bed was suitable for salmon spawning and egg deposition. To examine how streamflow and temperature parameter uncertainty influenced modeled outcomes, each scenario was simulated 1000 times using the same model parameters and uncertainty ranges used in the model sensitivity analysis. Model simulations were initialized with 100 spawners and run for 32 years, which allowed salmon populations to reach equilibrium in all scenarios. Results were presented as proportional change in abundance of returning salmon spawners relative to background conditions (i.e., no change in streamflow or thermal regime) using the same set of model parameters.

### Temporal data aggregation scenarios

We aggregated daily streamflow and thermal regime data for the glacier-, snow-, and rain-fed streams into weekly and monthly averages to examine how the temporal resolution of environmental data influenced modeled outcomes (Fig. 2). We aggregated regimes for the baseline condition, as well as for the most extreme scenario described above (100% increase in winter maximum flood magnitude, 100% decrease in summer minimum streamflow magnitude, and 40% increase in peak summer water temperature). Salmon spawner abundance from weekly and monthly simulations were then compared to responses produced from daily data. Weekly and monthly data aggregation was also done for the 23-year streamflow and thermal regime time series from Staney Creek, to examine the effects of data aggregation on the predicted dynamics of spawner abundance over this long-term period.

**Fig. 3.** Spawner-to-spawner relationships produced by the baseline life cycle model for glacier-, snow-, and rain-fed watersheds. The graph displays the number of spawning adult salmon offspring (*y*-axis) produced from a given number of parent spawners (*x*-axis) after a single lifecycle (4 years). Colored dots represent the equilibrium spawner abundance for each stream type after running the baseline model for 10 generations (40 years).

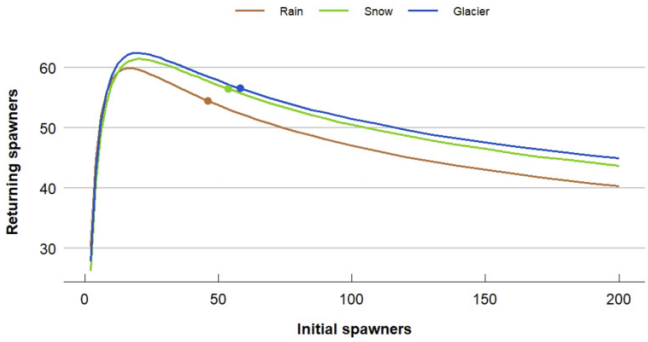


## Results

### Model validation and sensitivity analysis

The relationship between the number of parent spawners and adult spawning offspring in the baseline configuration of the life cycle model exhibited density dependence. The shapes of the modeled spawner-to-spawner curves were comparable to what might be expected for coho salmon populations in southeastern Alaska, which are typically managed using common fisheries recruitment models such as Ricker or Beverton-Holt (Fukushima et al. 1997; Barrowman et al. 2003). The ratio of adult spawning offspring to parent spawners increased sharply across low spawner densities (about 2–10 spawners/km) for all three stream types, peaking at 60–62 spawners/km (Fig. 3). After the peak, adult spawning offspring density decreased, to slightly varying degrees in each stream type, in response to larger numbers of parent spawners. After running the model to equilibrium in each stream type, the median number of adult offspring spawners/km was similar among glacier- (58 returning adults), snow- (54), and rain-fed (46) rivers (Fig. 3). These numbers are comparable to coho salmon spawner densities in southeastern Alaska and farther south in their range (Clark 1995; Bradford et al. 2000).

The life cycle model simulations were sensitive to uncertainty in four model parameters that explained nearly all the variation in spawner abundance (Fig. 4): (1) smolt length at which marine survival is 50% of the maximum, $HS_{smolt}$ (im-

**Fig. 4.** Relative importance of 11 model parameters to the baseline population abundance produced by the coho salmon life cycle model. Parameters are ranked according to those most important for glacier-fed watersheds.

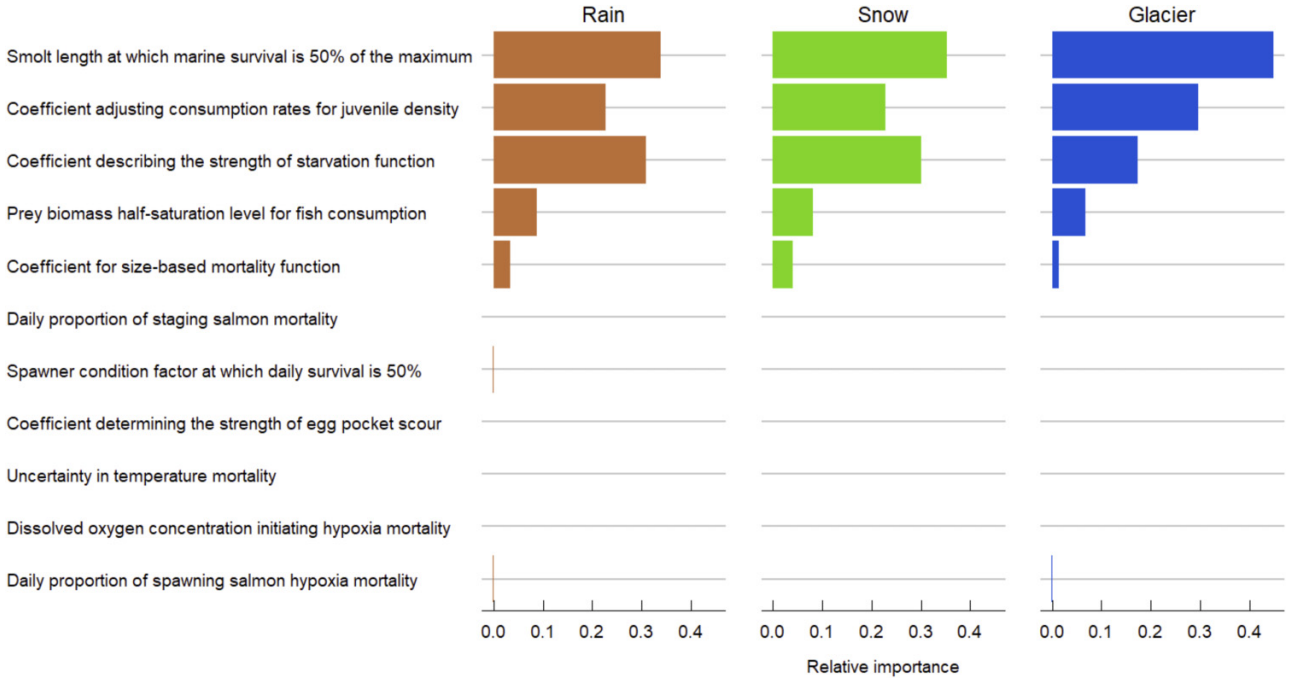


portance values ranged from 34% to 45%); (2) the coefficient adjusting consumption rates for juvenile density, $\gamma_Y$ (importance values ranged from 23% to 30%); (3) the coefficient describing the strength of the starvation function, $\alpha_{starve}$ (importance values ranged from 17% to 31%); and (4) prey biomass half-saturation level for fish consumption, $HS_{prey}$ (importance values ranged from 7% to 9%).

## Salmon population response to shifting streamflow and thermal regimes

The response of coho salmon populations to shifting streamflow and thermal regimes varied across modeled rain-, snow-, and glacier-fed streams (Fig. 5). Across all 17 scenarios, rain-fed streams exhibited the most variable and strongest population responses—from nearly no change relative to baseline salmon abundance to complete loss—whereas the population response of snow- and glacier-fed streams exhibited less dramatic population variability, and in some scenarios median salmon abundance slightly increased.

Higher magnitude winter floods that scour the streambed and kill incubating salmon embryos were associated with population declines in the rain- and snow-fed streams (Fig. 5). In the rain-fed stream, a winter flood increase of 50% resulted in a median decrease of 8% in salmon abundance, while winter flood increases of 75% and 100% resulted in 95% and 100% median decreases in abundance, respectively. In the snow-fed stream, decreases in salmon abundance were less severe; median decreases ranged from 1% to 6% across all four winter flood scenarios. In contrast, modeled salmon abundance in the glacier-fed stream was largely insensitive to increased winter floods, and median abundance was slightly higher (~1%) when winter floods were increased by 25% and 50% (Fig. 5). Variation in modeled responses between stream types was due to differences in baseline winter flood magnitudes, and the ability of compensatory density dependence during the juvenile life stage to counteract higher egg mortality. A 100% increase in flood magnitude resulted in 72% and 81% egg life stage mortality in the glacier- and snow-fed streams, respectively. Fewer eggs resulted in lower juvenile density, resulting in better juvenile growth and survival due to reduced density-dependence (Fig. 6). However, this same compensatory feedback could not overcome the high levels of egg mortality predicted to occur with increased flood magnitude in the rain-fed stream, where a 100% increase in flood magnitude resulted in 99% egg mortality and eliminated the salmon population.

In seven of the eight scenarios examining summer low flows or summer heat in isolation, there was surprisingly little change in salmon abundance (median change ranged from − 2% to + 1%; Fig. 5). The exception was an 11% to 20% decrease in median salmon abundance under the most extreme summer drought scenario (100% decrease in streamflow, but with isolated pools for 50% of channel length). In this scenario, low streamflow created substantially (>20 times) higher fish densities for a two-week period in the summer, which decreased juvenile growth and size and increased mortality due to greater density-dependent effects on foraging (see eq. 12; Fig. 6). Increases in summer water temperature without an accompanying decrease in streamflow never resulted in population declines, even when summer temperatures exceeded 20°C in the rain-fed stream in the most extreme temperature scenario (40% temperature increase; Fig. 5).

**Fig. 5.** Adult population response to flow and thermal regime modifications from base scenarios for rain (brown), snow (green), and glacier (blue) runoff watersheds. "Max. flow" and "Min. flow" refer to maximum and minimum instantaneous flows during the calendar year. Points on each line represent the median, ends of the thick lines represent 25th/75th percentiles, and ends of thin lines represent 5th/95th percentiles.

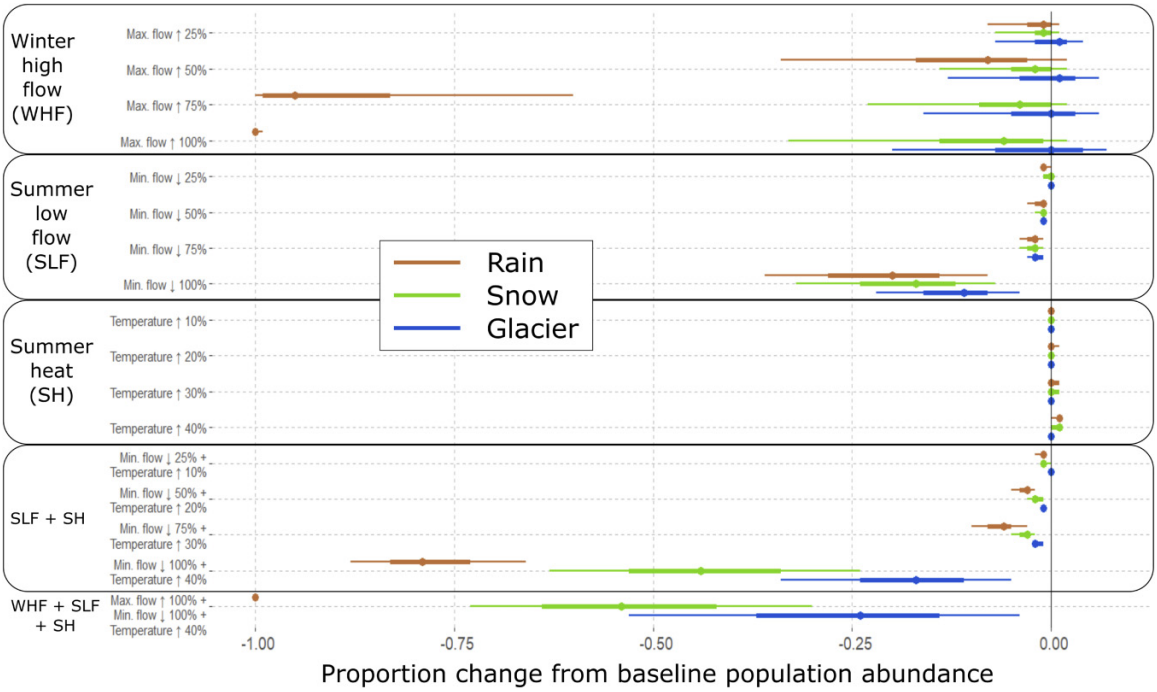


**Fig. 6.** Life cycle model mechanisms driving coho salmon population response to shifting environmental conditions. Symbols indicate whether each component increased (+) or decreased (−). As you follow the arrows, read "therefore," but against the arrows, read "because". In the winter high flow panel, fewer eggs may result in increased or decreased returning adult abundance depending on the magnitude of egg mortality and the ability for improved juvenile growth and survival to mitigate for egg losses (represented by the curved arrows).

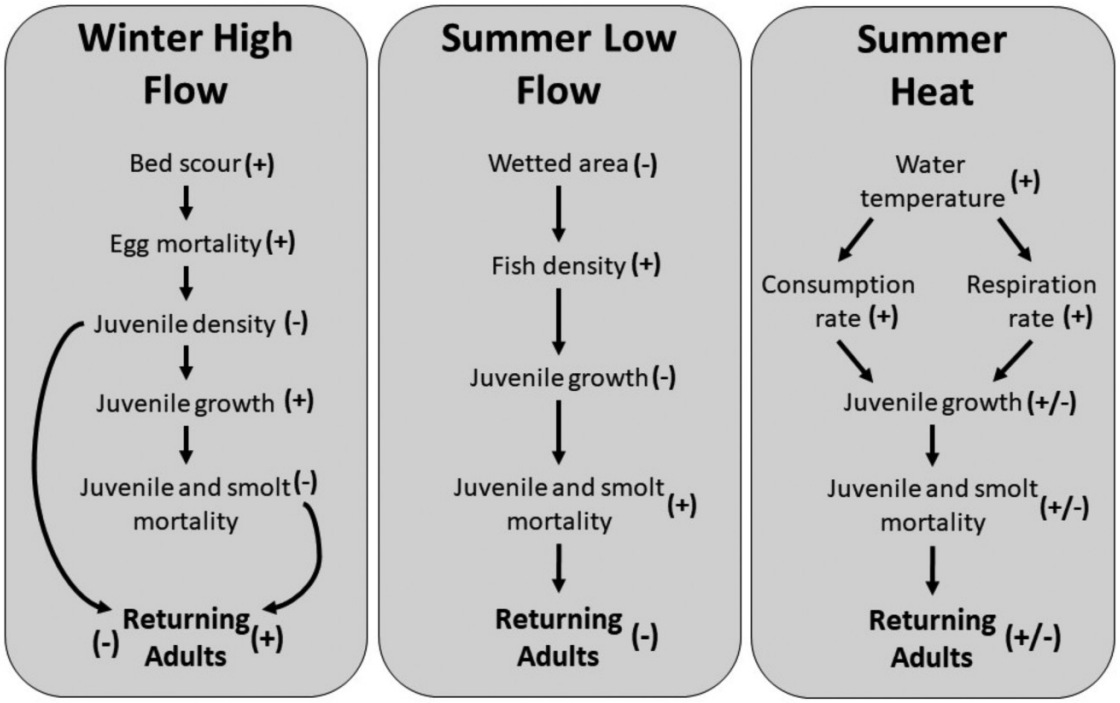

The combination of decreasing summer streamflow and increasing water temperature had an interactive and more substantial effect on median change in salmon abundance (Fig. 5). In the most extreme scenario (100% streamflow decrease, 40% temperature increase) salmon abundance decreased by a median of 79%, 44%, and 17% for rain-, snow-, and glacier-fed streams, respectively. These decreases were associated with greater juvenile respiration rates and lower food consumption rates (Fig. 6). Although warmer temperatures increased consumption rates, this was negated by lower streamflow that increased fish densities and created density-dependent effects on foraging. As a result, energy costs (respiration) for juvenile salmon exceeded energy intake (consumption), resulting in lower growth and greater starvation (Fig. 6). The final and most extreme scenario had the largest effect on populations due to the combined effects of winter flood (+100%), summer drought (−100%), and summer heat (+40%) (Fig. 5). In this scenario, median salmon abundance decreased by 100%, 54%, and 24% for rain-, snow-, and glacier-fed streams, respectively (Fig. 5).

### Changes in model results based on temporal data aggregation

The temporal resolution of streamflow and thermal regime data greatly influenced salmon population responses to the most extreme scenario (winter flood + 100%, summer drought − 100%, and summer heat + 40%). Aggregating daily streamflow and temperature time series into weekly and monthly averages (see Fig. 2) dampened the influence of short-duration flood and drought conditions in the model, which reduced predicted impacts on populations in all three stream types (Fig. 7). In the rain-fed stream, median salmon abundance decreases were 100%, 76%, and 51% for daily, weekly, and monthly time scales, respectively. Using the same time scale order, the snow-fed stream decreases were calculated as 54%, 36%, and 17%, and glacier-fed stream 24%, 14%, and 10%.

### Salmon population dynamics in Staney Creek

Using 23 years of daily streamflow and thermal regime data from rain-fed Staney Creek, modeled coho salmon annual abundance varied from 205 to 307 returning spawners/km, except for 2017 when the population dropped to 136 salmon/km (Fig. 8). The 2017 drop was associated with a flood event that occurred on 14 January 2014, when eggs from 2013 salmon spawners were still incubating in the stream gravel. The average modeled spawner return across years was 235 salmon/km using the daily data; aggregating the 23 year daily streamflow and temperature time-series into weekly and monthly averages increased the average returns to 294 and 318 salmon/km, respectively (Fig. 8). The largest disparity in modeled abundance occurred in 2017, when 136 returning spawners were predicted using daily data, 305 using weekly data, and 340 using monthly data (150% increase). Differences in 2017 returns were a result of dampening the 2014 high streamflow peak from 317.1 $m^3 s^{-1}$ (average daily value), to 55.6 $m^3 s^{-1}$ (weekly), to 18.8 $m^3 s^{-1}$ (monthly).

## Discussion

Using a process-based salmon life cycle model that integrates daily streamflow and water temperature data, our simulations illustrate that extreme floods and droughts can have deleterious effects on salmon populations in watersheds with similar flow and thermal regimes to those in southeastern Alaska. Among the three stream types we tested, salmon populations in rain-fed streams were the most sensitive to winter floods that increased egg mortality and drought conditions that concentrated salmon in warm, isolated pools. In comparison, salmon populations in the snow- and glacier-fed streams were relatively resilient to all but the most extreme flood and drought scenarios. These findings suggest that salmon abundance in lower-elevation rain-fed streams may become more variable year-to-year depending on the future frequency and severity of winter floods and summer droughts. In contrast, watersheds with snow and ice runoff—which are sometime considered to be less productive—are likely to serve as important future climate refugia for salmon (Pitman et al. 2020).

Relative to rain-fed watersheds of similar size, salmon rearing or spawning in many glacier- and snow-fed watersheds may be buffered from some extreme events for two reasons. First, the higher average elevation of snow- and glacier-fed watersheds may lead to more precipitation stored as snow in the watershed during autumn and winter months, thus decreasing peak flows relative to flashier rain-fed streams. Second, meltwaters keep streamflow higher, colder, and less variable in summer (Fellman et al. 2014; O'Neel et al. 2014), providing more water for salmon to feed, rear, migrate, and spawn. This dynamic played out during 2019 in Prince William Sound, Alaska, where many rain-fed watersheds experienced summer drought that inhibited upstream spawning migrations of Pacific salmon; but, these negative effects on upstream migration success were less common in snow- and glacier-fed watersheds (von Biela et al. 2022). Rain-fed watersheds numerically comprise around one-third of all watersheds in southern coastal Alaska (Sergeant et al. 2020); they are the most prone to drought, tend to experience maximum streamflow from December through May when salmon eggs are in their gravel nests, and tend to have the highest water temperatures in the region (Winfree et al. 2018; Sergeant et al. 2020). We note that we have not considered glacier lake outburst floods, which are predicted to increase in frequency in mountainous regions (Harrison et al. 2018), can be quite high in magnitude relative to other flood sources, and may be an important dynamic in larger glacier-fed watersheds (Carrivick and Tweed 2013).

The winter flood dynamics of watersheds such as those found in southern coastal Alaska are likely to become increasingly complicated in the future. Over the remainder of the 21st century, scientists expect snowline elevations to continue rising, which will shift the hydrology of many watersheds from primarily snow-fed to primarily rain-fed inputs (Beamer et al. 2017; Littell et al. 2018; Crumley et al. 2019). A rising snowline elevation also increases the potential for greater amounts of precipitation falling as rain during the winter. We hypothesize that some moderate elevation snow-

**Fig. 7.** The influence of temporal data aggregation on adult population response to flow and thermal regime modifications in the worst-case scenario for rain (brown), snow (green), and glacier (blue) runoff watersheds. "Max. flow" and "Min. flow" refer to maximum and minimum instantaneous flows during the calendar year. Points on each line represent the median, ends of the thick lines represent 25th/75th percentiles, and ends of thin lines represent 5th/95th percentiles.

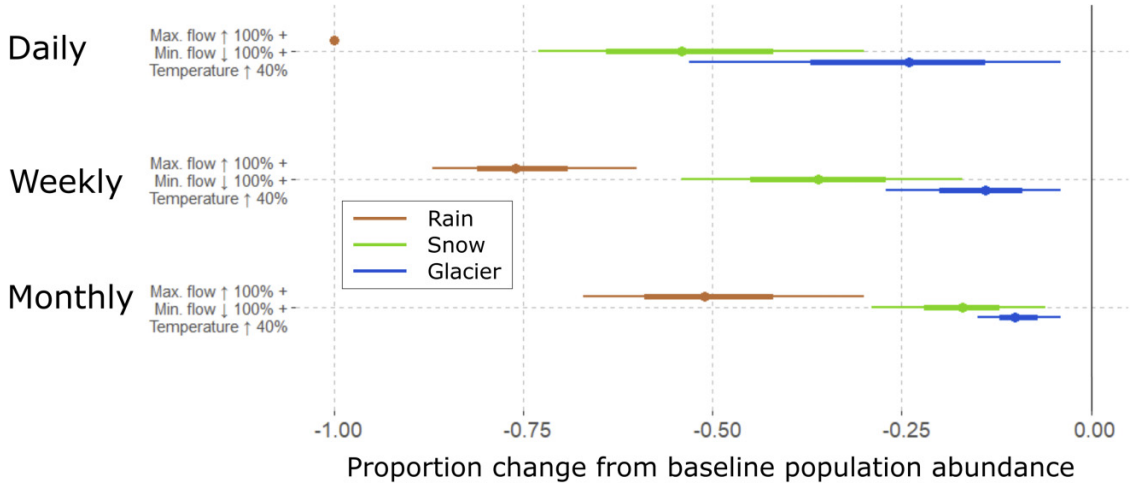


**Fig. 8.** Staney Creek model results from 1997 to 2019 vary by temporal aggregation of data. (A) Daily average discharge ($m^3/s$) from 1997 to 2019. (B) Daily average water temperature (°C) from 1997 to 2019. (C) Returning spawners/km by daily, weekly, and monthly data aggregation.

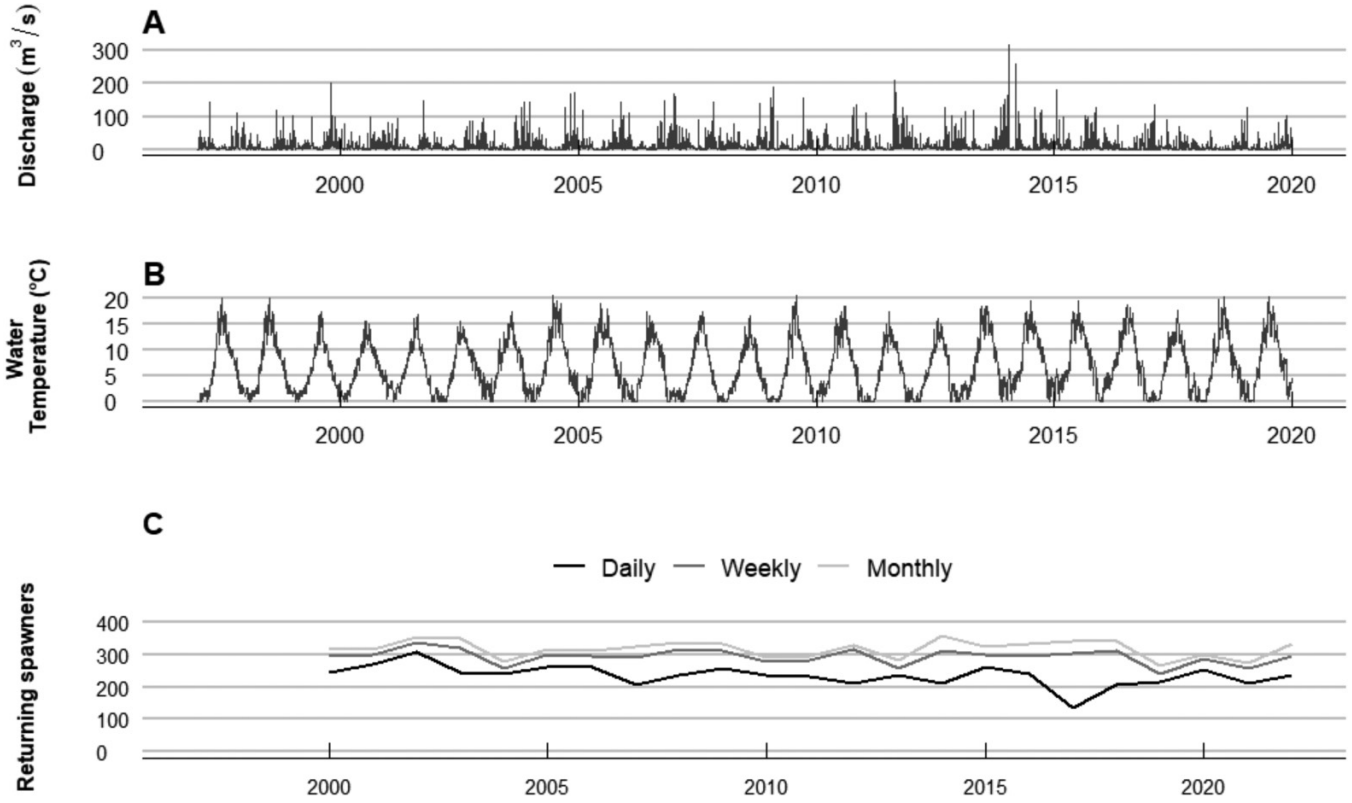


and glacier-fed watersheds may begin to experience larger rain-on-snow events than low elevation rain-fed watersheds depending on snow accumulation dynamics at low elevation (i.e., if no snow falls at low elevation, then no snow is available for a rain-on-snow event). In general, greater hydrologic homogenization of watersheds could mean that future salmon populations may be less resilient to extreme climate events.

A potentially surprising outcome of our analysis was that warming water temperatures, without concurrent changes in streamflow, had almost no impact on modeled population dynamics. Although there is a general expectation that

warming water temperatures will be harmful to coldwater fishes (Armstrong et al. 2021), temperatures in most southeastern Alaska watersheds are well below harmful physiological thresholds for salmon. Water temperatures do exceed 20°C in some of the warmest streams, but some streams' temperatures are still considered sub-optimally cold for juvenile salmon growth (Bellmore and Winfree 2019). While warmer waters may increase juvenile salmon growth, they may also result in higher disease risk, shifting patterns of food availability, and increased presence of predators and competitors (Mauger et al. 2017), which we do not account for in this model. These conflicting factors complicate predictions on the future implications of warming temperatures for salmon in coastal Alaska. Warmer water temperatures typically correspond with periods of low streamflow (Caissie 2006), which our model suggests is likely to negatively impact salmon populations. Discussions of the negative impacts of warming water temperature must carefully differentiate between salmon populations in the northern versus southern portions of their range, where water temperatures can increase to more than 30°C (Fitzgerald and Martin 2022).

## Implications of temporal data aggregation on modeling salmon abundance

Aggregating data at coarser temporal resolution (weekly and monthly) demonstrated that daily streamflow and water temperature data were critical to detecting and interpreting the impacts of floods and droughts. In southeastern Alaska, a region that generally lacks extensive periods of record for daily-scale hydrologic and temperature data, these findings emphasize the importance of collecting high-resolution measurements in watersheds that are at greatest risk for extreme events in the future (Mauger et al. 2017; Sloat et al. 2017). Although continuous monitoring of ecosystems is becoming more common with newer technology such as smaller temperature loggers with long battery life and abundant memory, predicting how populations and ecosystems will respond also requires high-resolution modeling tools that can fully utilize these environmental data. The efficacy of these tools will also hinge on the availability of downscaled predictions of how extreme conditions are expected to change in the future at finer scales of time and space.

Even when high-resolution data are available, many population models are parameterized with data that are averaged across months or entire life-stages (e.g., Scheuerell et al. 2006; Crozier et al. 2008), which is likely to mask the impacts of short-duration extreme events. In many salmon life cycle models, for instance, success at a given life stage is often a function of the average environmental conditions (e.g., temperature, habitat area, density dependence, etc.) experienced during that life stage (e.g., Crozier et al. 2008; Leppi et al. 2014). Although these approaches may adequately represent generalizable environmental trends that occur at longer time scales (e.g., earlier snowmelt runoff peaks and lower baseflows), our results suggest that models that aggregate data at weekly or greater time scales may be insufficient to evaluate the importance of extreme and stochastic events—especially in freshwater habitats that are already stochastic (e.g., rain-fed streams found across the Northeast Pacific Coastal Temperate Rainforest; Bidlack et al. 2021). Linking population dynamics to high-resolution data may require process-based models, such as ours, that mechanistically link the success of cohorts or individuals to short-term environmental conditions (other examples include Perry et al. 2019 and Railsback et al. 2013).

## Model limitations and future applications

Several simplifications may limit the inferences gained from our life cycle model. Some of the processes known to influence salmon populations but not represented include: (1) variation in individual life histories (Quinn 2018), (2) effects of streamflow and water temperature on food availability and foraging success (Rossi et al. 2021), (3) interactions with other fish species that compete with and prey upon juvenile salmon (Bellmore et al. 2013), and (4) spatial heterogeneity and movement of individuals within stream networks (Armstrong and Schindler 2013; Railsback et al. 2013; Fullerton et al. 2017; Beechie et al. 2021; Jorgensen et al. 2021). We acknowledge that these complexities are important and hope that our model provides a framework for future analyses that address the above omissions. For example, our life cycle model could be linked to existing river food web models (e.g., Bellmore et al. 2017) to account for the unique food web dynamics of glacier-, snow-, and rain-fed streams (Bellmore et al. 2022). Future applications could also include expanding the model to other regions and species that experience flood and drought impacts differently. Pink and chum salmon, for instance, frequently spawn during summer months when adults may be more susceptible to drought conditions creating hypoxia (Sergeant et al. 2017; Tillotson and Quinn 2017; von Biela et al. 2022). A hypoxia mortality process was included in our model but was not triggered since coho salmon spawned in October when flows were higher.

Future analyses would also benefit from more precise estimates of model parameters. Uncertainty in the value of model parameters translated into substantial uncertainty in population responses to several flood and drought scenarios (Fig. 5). Our sensitivity analysis pointed to the need for more accurate estimates of model parameters linked to juvenile and smolt survival (Fig. 4). Future analyses could also incorporate model uncertainty using different approaches. We conducted simulations using a deterministic approach that is useful for understanding model behavior. In future applications, incorporating model uncertainty using a stochastic approach, whereby parameter values vary year-to-year, may provide more realistic expectations about the variability in population abundance through time.

An important next step is to apply the model to southeastern Alaska watersheds that support salmon harvests and are critical to community well-being. There is a growing network of community-collected stream temperature data in the region (Bellmore and Winfree 2019), which could be combined with modeled streamflow data (e.g., Yang

et al. 2021) to parameterize the life cycle model for specific watersheds and populations. User-friendly model interfaces could also be constructed that would allow community members and local managers to parameterize and run the model on their own (see our online Salmon Simulator at https://exchange.iseesystems.com/public/ryan-bellmore/salmon-life-cycle-simulator/). Subsequent simulations could facilitate adaptation and scenario planning in the region by identifying communities that rely on salmon stocks that may be highly sensitive to future changes in streamflow and temperature.

## Conclusions

Our analysis supports previous studies demonstrating that salmon populations are strongly impacted by shifting freshwater conditions (Holtby et al. 1989; Bradford 1995; Neuswanger et al. 2015; Jones et al. 2020; Gibeau and Palen 2021; Warkentin et al. 2022; Wilson et al. 2022). We add to this literature by illustrating that short-duration extreme events, lasting only a few days, can strongly control population dynamics. However, responses to these extremes are likely to play out differently across the thousands of glacier-, snow-, and rain-fed watersheds in southeastern Alaska and other portions of the Northeast Pacific Coastal Temperate Rainforest (Sergeant et al. 2020; Bidlack et al. 2021), which collectively represent a diverse portfolio of biophysical conditions and associated responses to climate change. While at a regional scale there may be species-specific population stability across this diverse set of watersheds, our findings emphasize that more severe floods and droughts may destabilize some salmon populations at local scales. However, coarse scale population models with monthly, seasonal, or annual time steps are likely to underestimate the impacts of short-duration extreme events. Our analysis suggests that predicting how individual salmon populations will respond to extremes will require models, like the one presented here, that operate at finer temporal scales and better align with the scale of environmental variability that freshwater species experience.

## Acknowledgements

This research was supported by Alaska Sea Grant (project R/31-25). F. Mueter provided a preliminary review of the original manuscript. P. Westley and D. Holen provided preliminary input on the approach and application of our work. J. Sowa provided discharge data. We thank two anonymous reviewers for constructive comments that improved the final manuscript.

## Article information

### History dates

Received: 18 June 2022
Accepted: 9 September 2022
Accepted manuscript online: 4 October 2022
Version of record online: 6 January 2023

### Copyright



### Data availability statement

Data generated or analyzed during this study are provided in full within the published article and its supplementary materials.

## Author information

### Author ORCIDs

Christopher J. Sergeant https://orcid.org/0000-0002-3363-3213

### Author notes

J. R. Bellmore and C. J. Sergeant should be considered joint first author.

### Author contributions

Conceptualization: JRB, CJS, RAB, JAF
Data curation: JRB, CJS, RAB, JBF
Formal analysis: JRB, CJS, RAB
Funding acquisition: JRB, CJS
Investigation: JRB, CJS, RAB, JAF
Methodology: JRB, CJS, RAB, JAF, JBF
Project administration: JAF
Supervision: JAF
Visualization: JRB, CJS
Writing – original draft: JRB, CJS, RAB, JAF
Writing – review & editing: JRB, CJS, RAB, JAF, JBF

### Competing interests

The authors declare there are no competing interests.

## Supplementary material

Supplementary data are available with the article at https://doi.org/10.1139/cjfas-2022-0129.

## References

Adrian, R., Gerten, D., Huber, V., Wagner, C., and Schmidt, S.R. 2012. Windows of change: temporal scale of analysis is decisive to detect ecosystem responses to climate change. Mar. Biol. **159**(11): 2533–2542. doi:10.1007/s00227-012-1938-1.

Armstrong, J.B., Fullerton, A.H., Jordan, C.E., Ebersole, J.L., Bellmore, J.R. Arismendi, I., et al. 2021. The importance of warm habitat to the growth regime of cold-water fishes. Nat. Clim. Chang. **11**(4): 354–361. doi:10.1038/s41558-021-00994-y. PMID: 35475125.

Armstrong, J.B., and Schindler, D.E. 2013. Going with the flow: spatial distributions of juvenile coho salmon track an annually shifting mosaic of water temperature. Ecosystems **16**(8): 1429–1441. doi:10.1007/s10021-013-9693-9.

Augerot, X., and Foley, D. 2005. *Atlas of Pacific Salmon: The First Map-Based Status Assessment of Salmon in the North Pacific*. University of California Press, Berkeley, CA.

Barrowman, N.J., Myers, R.A., Hilborn, R., Kehler, D.G., and Field, C.A. 2003. The variability among populations of coho salmon in the maximum reproductive rate and depensation. Ecol. Appl. **13**(3): 784–793. doi:10.1890/1051-0761(2003)013[0784:TVAPOC]2.0.CO;2.

Beacham, T.D., and Murray, C.B. 1990. Temperature, egg size, and development of embryos and alevins of five species of pacific salmon: a comparative analysis. Trans. Am. Fish. Soc. **119**(6): 927–945. doi:10.1577/1548-8659(1990)119⟨0927:tesado⟩2.3.co;2.

Beamer, J.P., Hill, D.F., McGrath, D., Arendt, A., and Kienholz, C. 2017. Hydrologic impacts of changes in climate and glacier extent in the gulf of Alaska watershed. Water Resour. Res. **53**(9): 7502–7520. doi:10.1002/2016WR020033.

Beechie, T.J., Nicol, C., Fogel, C., Jorgensen, J., Thompson, J. Seixas, G., et al. 2021. *Modeling Effects of Habitat Change and Restoration Alternatives on Salmon in the Chehalis River Basin using a Salmonid Life-Cycle Model*. NOAA Contract Report NMFS-NWFSC-CR-2021-01. U.S. Department of Commerce, Seattle, WA.

Bellmore, J.R., Baxter, C. V., Martens, K., and Connolly, P.J. 2013. The floodplain food web mosaic: a study of its importance to salmon and steelhead with implications for their recovery. Ecol. Appl. **23**(1): 189–207. doi:10.1890/12-0806.1. PMID: 23495646.

Bellmore, J.R., Benjamin, J.R., Newsom, M., Bountry, J.A., and Dombroski, D. 2017. Incorporating food web dynamics into ecological restoration: a modeling approach for river ecosystems. Ecol. Appl. **27**(3): 814–832. doi:10.1002/eap.1486. PMID: 28078716.

Bellmore, J.R., Fellman, J.B., Hood, E., Dunkle, M.R., and Edwards, R.T. 2022. A melting cryosphere constrains fish growth by synchronizing the seasonal phenology of river food webs. Glob. Chang. Biol. **28**(16): 4807–4818. doi:10.1111/gcb.16273. PMID: 35596718.

Bellmore, R., and Winfree, M. 2019. Southeast alaska freshwater monitoring network implementation plan. Available from: https://acrc.alaska.edu/docs/streamtemp-implementationplan.pdf [accessed 3 September 2022].

Benda, L., Miller, D., Andras, K., Bigelow, P., Reeves, G., and Michael, D. 2007. NetMap: a new tool in support of watershed science and resource management. For. Sci. **53**(2): 206–219. doi:10.1093/forestscience/53.2.206.

Benda, L., Miller, D., Barquin, J., McCleary, R., Cai, T.J., and Ji, Y. 2016. Building virtual watersheds: a global opportunity to strengthen resource management and conservation. Environ. Manag. **57**(3): 722–739. doi:10.1007/s00267-015-0634-6. PMID: 26645078.

Benjamin, J.R., Bellmore, J.R., Whitney, E., and Dunham, J.B. 2020. Can nutrient additions facilitate recovery of pacific salmon? Can. J. Fish. Aquat. Sci. **77**(10): 1601–1611. doi:10.1139/cjfas-2019-0438.

Benson, B.B., and Krause, J.D. 1980. The concentration and isotopic fractionation of gases dissolved in freshwater in equilibrium with the atmosphere. 1. Oxygen. Limnol. Oceanogr. **25**(4): 662–671. doi:10.4319/lo.1980.25.4.0662.

Bidlack, A.L., Bisbing, S.M., Buma, B.J., Diefenderfer, H.L., Fellman, J.B. Floyd, W.C., et al. 2021. Climate-mediated changes to linked terrestrial and marine ecosystems across the northeast pacific coastal temperate rainforest margin. Bioscience **71**(6): 581–595. doi:10.1093/biosci/biaa171.

von Biela, V.R., Sergeant, C.J., Carey, M.P., Liller, Z., Russell, C. Quinn-Davidson, S., et al. 2022. Premature mortality observations among Alaska's pacific salmon during record heat and drought in 2019. Fisheries **47**(4): 157–168. doi:10.1002/fsh.10705.

Biles, F. 2016. A continuous, transboundary, 50-meter DEM for alaska perhumid coastal temperate rainforest (AKPCTR_DEM). U.S. Geological Survey, Science-Base Catalog, Virginia, USA, Available from https://www.sciencebase.gov/catalog/item/580018b5e4b0824b2d179da4 [accessed 3 September 2022].

Biles, F. 2019. USFS Southeast Alaska drainage basin (SEAKDB) watersheds. State of Alaska, Open Data Geoportal, Juneau, Alaska, USA, Available from: https://gis.data.alaska.gov/datasets/6f9e00ba416c4f34a7f2f96cc411ef47/about [accessed 3 September 2022].

Bjornn, T.C., and Reiser, D.W. 1991. Habitat requirements of salmonids in streams. *In Influences of Forest and Rangeland Management on Salmonid Fishes and Their Habitats. Edited by* W.R. Meehan. American Fisheries Society Special Publication 19. pp. 83–138. doi:10.2307/1446234.

Bowerman, T., Roumasset, A., Keefer, M.L., Sharpe, C.S., and Caudill, C.C. 2018. Prespawn mortality of female Chinook salmon increases with water temperature and percent hatchery origin. Trans. Am. Fish. Soc. **147**(1): 31–42. doi:10.1002/tafs.10022.

Bradford, M.J. 1995. Comparative review of pacific salmon survival rates. Can. J. Fish. Aquat. Sci. **52**(6): 1327–1338. doi:10.1139/f95-129.

Bradford, M.J., Myers, R.A., and Irvine, J.R. 2000. Reference points for coho salmon (*Oncorhynchus kisutch*) harvest rates and escapement goals based on freshwater production. Can. J. Fish. Aquat. Sci. **57**(4): 677–686. doi:10.1139/f99-281.

Caissie, D. 2006. The thermal regime of rivers: a review. Freshw. Biol. **51**(8): 1389–1406. doi:10.1111/j.1365-2427.2006.01597.x.

Carrivick, J.L., and Tweed, F.S. 2013. Proglacial lakes: character, behaviour and geological importance. Quat. Sci. Rev. **78**: 34–52. doi:10.1016/j.quascirev.2013.07.028.

Clark, J.H. 1995. Escapement goals for coho salmon stocks returning to streams located along the Juneau road system of Southeast Alaska. Alaska Department of Fish and Game, Regional Information Report 1J95-02, Juneau, Alaska.

Crozier, L.G., Zabel, R.W., and Hamlet, A.F. 2008. Predicting differential effects of climate change at the population level with life-cycle models of spring Chinook salmon. Glob. Chang. Biol. **14**(2): 236–249. doi:10.1111/j.1365-2486.2007.01497.x.

Crumley, R.L., Hill, D.F., Beamer, J.P., and Holzenthal, E.R. 2019. Seasonal components of freshwater runoff in Glacier Bay, Alaska: diverse spatial patterns and temporal change. Cryosphere **13**: 1597–1619. doi:10.5194/tc-2019-1.

Cunningham, C.J., Westley, P.A.H., and Adkison, M.D. 2018. Signals of large scale climate drivers, hatchery enhancement, and marine factors in Yukon river Chinook salmon survival revealed with a Bayesian life history model. Glob. Chang. Biol. **24**(9): 4399–4416. doi:10.1111/gcb.14315. PMID: 29774975.

Deslauriers, D., Chipps, S.R., Breck, J.E., Rice, J.A., and Madenjian, C.P. 2017. Fish bioenergetics 4.0: an R-Based modeling application. Fisheries **42**(11): 586–596. doi:10.1080/03632415.2017.1377558.

Easterling, D.R., Meehl, G.A., Parmesan, C., Changnon, S.A., Karl, T.R., and Mearns, L.O. 2000. Climate extremes: observations, modeling, and impacts. Science **289**(5487): 2068–2075. doi:10.1126/science.289.5487.2068. PMID: 11000103.

Elmore, H.L., and West, W.F. 1961. Effects of water temperature on stream sanitation. J. Sanit. Eng. Div. **87**(6): 59–71. ASCE.

English, K.K., Bocking, R.C., and Irvine, J.R. 1992. A robust procedure for estimating salmon escapement based on the area-under-the-curve method. Can. J. Fish. Aquat. Sci. **49**(10): 1982–1989. doi:10.1139/f92-220.

Fellman, J.B., Nagorski, S., Pyare, S., Vermilyea, A.W., Scott, D., and Hood, E. 2014. Stream temperature response to variable glacier coverage in coastal watersheds of Southeast Alaska. Hydrol. Process. **28**(4): 2062–2073. doi:10.1002/hyp.9742.

Fitzgerald, A.M., and Martin, B.T. 2022. Quantification of thermal impacts across freshwater life stages to improve temperature management for anadromous salmonids. Conserv. Physiol. **10**(1): 1–17. doi:10.1093/conphys/coac013.

Ford, A. 2009. *Modeling the Environment*, 2nd Edition. Island Press, Washington, DC.

Fukushima, M., Taylor, S.G., and Smoker, W.W. 1997. Fry and smolt production of pink and sockeye salmon in the Auke Lake system, Southeast Alaska. Acta Hydrobiol. Sin. **21**: 1–21.

Fullerton, A.H., Burke, B.J., Lawler, J.J., Torgersen, C.E., Ebersole, J.L., and Leibowitz, S.G. 2017. Simulated juvenile salmon growth and phenology respond to altered thermal regimes and stream network shape. Ecosphere, **8**(12): e02052. doi:10.1002/ecs2.2052.

Gibeau, P., and Palen, W.J. 2021. Impacts of run-of-river hydropower on coho salmon (*Oncorhynchus kisutch*): the role of density-dependent survival. Ecosphere, **12**(8): e03684. doi:10.1002/ecs2.3684.

Goode, J.R., Buffington, J.M., Tonina, D., Isaak, D.J., Thurow, R.F. Wenger, S., et al. 2013. Potential effects of climate change on streambed scour and risks to salmonid survival in snow-dominated mountain basins. Hydrol. Process. **27**(5): 750–765. doi:10.1002/hyp.9728.

Gordon, N.D., McMahon, T.A., Finlayson, B.L., Gippel, C.J., and Nathan, R.J. 2004. *Stream Hydrology: An Introduction for Ecologists*, 2nd Edition. John Wiley & Sons, West Sussex, England.

Grimm, N.B., and Fisher, S.G. 1989. Stability of periphyton and macroinvertebrates to disturbance by flash floods in a desert stream. J. North Am. Benthol. Soc. **8**(4): 293–307. doi:10.2307/1467493.

Hanson, P.C., Johnson, T.B., Schindler, D.E., and Kitchell, J.F. 1997. *Fish Bioenergetics 3.0*. University of Wisconsin Sea Grant Institute, Madison, Wisconsin.

Harper, E.B., Stella, J.C., and Fremier, A.K. 2011. Global sensitivity analysis for complex ecological models: a case study of riparian cottonwood population dynamics. Ecol. Appl. **21**(4): 1225–1240. doi:10.1890/10-0506.1. PMID: 21774426.

Harrison, S., Kargel, J.S., Huggel, C., Reynolds, J., Shugar, D.H. Betts, R.A., et al. 2018. Climate change and the global pattern of moraine-dammed glacial lake outburst floods, Cryosphere **12**: 1195–1209. doi:10.5194/tc-12-1195-2018.

Hetrick, N.J., and Nemeth, M.J. 2003. Survey of coho salmon runs on the pacific coast of the Alaska Peninsula and Becharof national wildlife refuges, 1994 with estimates of escapement for two small streams in 1995 and 1996. United State Fish and Wildlife Service, Alaska Fisheries Technical Report Number 63. King Salmon, Alaska.

Holtby, L.B., McMahon, T.E., and Scrivener, J.C. 1989. Stream temperatures and inter-annual variability in the emigration timing of coho salmon smolts and fry and chum salmon fry from carnation creek, British Columbia. Can. J. Fish. Aquat. Sci. **46**: 1396–1405. doi:10.1139/f89-179.

Holtgrieve, G.W., and Schindler, D.E. 2011. Marine-derived nutrients, bioturbation, and ecosystem metabolism: reconsidering the role of salmon in streams. Ecology **92**(2): 373–385. doi:10.1890/09-1694.1. PMID: 21618917.

Johnson, A.C., Bellmore, J.R., and Haught, S. 2019. Quantifying the monetary value of Alaska national forests to commercial pacific salmon fisheries. North Am. J. Fish. Manag. **39**(6): 1119–1131. doi:10.1002/nafm.10364.

Jones, L.A., Schoen, E.R., Shaftel, R., Cunningham, C.J., Mauger, S., Rinella, D.J., and St. Saviour, A. 2020. Watershed-scale climate influences productivity of Chinook salmon populations across south-central Alaska. Glob. Chang. Biol. **26**(9): 4919–4936. doi:10.1111/gcb.15155. PMID: 32628814.

Jorgensen, J.C., Nicol, C., Fogel, C., and Beechie, T.J. 2021. Identifying the potential of anadromous salmonid habitat restoration with life cycle models. PLoS ONE **16**(9): e0256792. doi:10.1371/journal.pone.0256792. PMID: 34499669.

Lamb, M.P., Dietrich, W.E., and Venditti, J.G. 2008. Is the critical shields stress for incipient sediment motion dependent on channel-bed slope? J. Geophys. Res. Earth Surf. **113**(2): 1–20. doi:10.1029/2007JF000831.

Ledger, M.E., and Milner, A.M. 2015. Extreme events in running waters. Freshw. Biol. **60**(12): 2455–2460. doi:10.1111/fwb.12673.

Leppi, J.C., Rinella, D.J., Wilson, R.R., and Loya, W.M. 2014. Linking climate change projections for an Alaskan watershed to future coho salmon production. Glob. Chang. Biol. **20**(6): 1808–1820. doi:10.1111/gcb.12492. PMID: 24323577.

Liaw, A., and Wiener, M. 2002. Classification and regression by randomForest. R News, **2**(3): 18–22.

Littell, J.S., McAfee, S.A., and Hayward, G.D. 2018. Alaska snowpack response to climate change: statewide snowfall equivalent and snowpack water scenarios. Water, **10**(5): 668. doi:10.3390/w10050668.

Lum, J.L. 2003. *Effects of Smolt Length and Emigration Timing on Marine Survival and Age at Maturity of Wild Coho Salmon (Oncorhynchus kisutch) at Auke Creek*, Master's Thesis, University of Alaska Fairbanks, Juneau, Alaska.

Mauger, S., Shaftel, R., Leppi, J.C., and Rinella, D.J. 2017. Summer temperature regimes in southcentral Alaska streams: watershed drivers of variation and potential implications for pacific salmon. Can. J. Fish. Aquat. Sci. **74**(5): 702–715. doi:10.1139/cjfas-2016-0076.

Maunder, M.N. 1997. Investigation of density dependence in salmon spawner-egg relationships using queueing theory. Ecol. Model. **104**(2–3): 189–197. doi:10.1016/S0304-3800(97)00126-9.

McCabe, G.J., Clark, M.P., and Hay, L.E. 2007. Rain-on-snow events in the western United States. Bull. Am. Meteorol. Soc. **88**(3): 319–328. doi:10.1175/BAMS-88-3-319.

McKay, M.D., Beckman, R.J., and Conover, W.J. 1979. A comparison of three methods for selecting values of input variables in the analysis of output from a computer code. Technometrics, **21**: 239–245. doi:10.1080/00401706.2000.10485979.

Milner, A.M., Robertson, A.L., McDermott, M.J., Klaar, M.J., and Brown, L.E. 2013. Major flood disturbance alters river ecosystem evolution. Nat. Clim. Chang. **3**(2): 137–141. doi:10.1038/nclimate1665.

Montgomery, D.R., Buffington, J.M., Peterson, N.P., Schuett-Hames, D., and Quinn, T.P. 1996. Stream-bed scour, egg burial depths, and the influence of salmonid spawning on bed surface mobility and embryo survival. Can. J. Fish. Aquat. Sci. **53**(5): 1061–1070. doi:10.1139/f96-028.

Murphy, M.L. 1985. Die-offs of pre-spawn adult pink salmon and chum salmon in southeastern Alaska. North Am. J. Fish. Manag. **5**(2B): 302–308. doi:10.1577/1548-8659(1985)5⟨302:DOPAPS⟩2.0.CO;2.

Nadeau, C.P., Urban, M.C., and Bridle, J.R. 2017. Coarse climate change projections for species living in a fine-scaled world. Glob. Change Biol. **23**(1): 12–24. doi:10.1111/gcb.13475.

Neuswanger, J.R., Wipfli, M.S., Evenson, M.J., Hughes, N.F., and Rosenberger, A.E. 2015. Low productivity of Chinook salmon strongly correlates with high summer stream discharge in two Alaskan rivers in the Yukon drainage. Can. J. Fish. Aquat. Sci. **72**: 1125–1137. doi:10.1139/cjfas-2014-0498.

O'Neel, S., Hood, E., Arendt, A., and Sass, L. 2014. Assessing streamflow sensitivity to variations in glacier mass balance. Clim. Change **123**(2): 329–341. doi:10.1007/s10584-013-1042-7.

O'Neel, S., Hood, E., Bidlack, A.L., Fleming, S.W., Arimitsu, M.L. Arendt, A., et al. 2015. Icefield-to-ocean linkages across the northern pacific coastal temperate rainforest ecosystem. Bioscience, **65**(5): 499–512. doi:10.1093/biosci/biv027.

Omerod, S.J. 2009. Climate change, river conservation and the adaptation challenge. Aquat. Conserv. Mar. Freshw. Ecosyst. **19**: 609–613. doi:10.1002/aqc.

Owens, M., Edwards, R.W., and Gibbs, J.W. 1964. Some reaeration studies in streams. Int. J. Air Water Pollut. **8**: 469–486.

Perry, R.W., Plumb, J.M., Jones, E.C., Som, N.A., Hardy, T.B., and Hetrick, N.J. 2019. *Application of the Stream Salmonid Simulator (S3) to Klamath River Fall Chinook Salmon (Oncorhynchus tshawytscha), California—Parameterization and Calibration*. United States Geological Survey, Open-File Report 2019-1107. Reston, VA.

Pitman, K.J., Moore, J.W., Sloat, M.R., Beaudreau, A.H., Bidlack, A.L. Brenner, R.E., et al. 2020. Glacier retreat and pacific salmon. Bioscience, **70**(3): 220–236. doi:10.1093/biosci/biaa015. PMID: 32174645.

Poff, N.L., Allan, J.D., Bain, M.B., Karr, J.R., Prestegaard, K.L. Richter, B.D., et al. 1997. The natural flow regime. Bioscience, **47**(11): 769–784. doi:10.2307/1313099.

Quinn, T.P. 2018. *The Behavior and Ecology of Pacific Salmon and Trout*, 2nd Edition. University of Washington Press, Seattle, WA.

R Core Team. 2019. *R: A Language and Environment for Statistical Computing*. R Foundation for Statistical Computing, Vienna, Austria. Available from: http://www.R-project.org/.

Radić, V., Cannon, A.J., Menounos, B., and Gi, N. 2015. Future changes in autumn atmospheric river events in British Columbia, Canada, as projected by CMIP5 global climate models. J. Geophys. Res. Atmos. **120**: 9279–9302. doi:10.1002/2015JD023279.

Railsback, S.F., Gard, M., Harvey, B.C., White, J.L., and Zimmerman, J.K.H. 2013. Contrast of degraded and restored stream habitat using an individual-based salmon model. N. Am. J. Fish. Manag. **33**(2): 384–399. doi:10.1080/02755947.2013.765527.

Railsback, S.F., Harvey, B.C., Jackson, S.K., and Lamberson, R.H. 2009. *InSTREAM: The Individual-Based Stream Trout Research and Environmental Assessment Model*. United States Forest Service, Pacific Southwest Research Station, General Technical Report, PSW-GTR-218. Albany, CA.

Rossi, G.J., Power, M.E., Pneh, S., Neuswanger, J.R., and Caldwell, T.J. 2021. Foraging modes and movements of *oncorhynchus mykiss* as flow and invertebrate drift recede in a California stream. Can. J. Fish. Aquat. Sci. **78**(8): 1045–1056. doi:10.1139/cjfas-2020-0398.

Sayre, R., Karagulle, D., Frye, C., Boucher, T., Wolff, N.H. Breyer, S., et al. 2020. An assessment of the representation of ecosystems in global protected areas using new maps of world climate regions and world ecosystems. Glob. Ecol. Conserv. **21**: e00860. Elsevier Ltd. doi:10.1016/j.gecco.2019.e00860.

Scheuerell, M.D., Hilborn, R., Ruckelshaus, M.H., Bartz, K.K., Lagueux, K.M., Haas, A.D., and Rawson, K. 2006. The Shiraz model: a tool for incorporating anthropogenic effects and fish-habitat relationships in conservation planning. Can. J. Fish. Aquat. Sci. **63**(7): 1596–1607. doi:10.1139/F06-056.

Schindler, D.E., Hilborn, R., Chasco, B., Boatright, C.P., Quinn, T.P., Rogers, L.A., and Webster, M.S. 2010. Population diversity and the portfolio effect in an exploited species. Nature **465**(7298): 609–612. doi:10.1038/nature09060.

Sergeant, C.J., Bellmore, J.R., McConnell, C., and Moore, J.W. 2017. High salmon density and low discharge create periodic hypoxia in coastal rivers. Ecosphere **8**(6): e01846. doi:10.1002/ecs2.1846.

Sergeant, C.J., Falke, J.A., Bellmore, R.A., Bellmore, J.R., and Crumley, R.L. 2020. A classification of streamflow patterns across the coastal Gulf of Alaska. Water Resour. Res. **56**(2): e2019WR026127. doi:10.1029/2019WR026127.

Shaftel, R., Mauger, S., Falke, J., Rinella, D., Davis, J., and Jones, L. 2020. Thermal diversity of salmon streams in the Matanuska-susitna Basin, Alaska. J. Am. Water Resour. Assoc. **56**(4): 630–646. doi:10.1111/1752-1688.12839.

Shanley, C.S., Pyare, S., Goldstein, M.I., Alaback, P.B., Albert, D.M. Beier, C.M., et al. 2015. Climate change implications in the northern coastal temperate rainforest of North America. Clim. Chang. **130**(2): 155–170. doi:10.1007/s10584-015-1355-9.

Sharma, A.R., and Déry, S.J. 2020. Contribution of atmospheric rivers to annual, seasonal, and extreme precipitation across British Columbia and Southeastern Alaska. J. Geophys. Res. Atmos. **125**(9): e2019JD031823. doi:10.1029/2019JD031823.

Sloat, M.R., Reeves, G.H., and Christiansen, K.R. 2017. Stream network geomorphology mediates predicted vulnerability of anadromous fish habitat to hydrologic change in southeast Alaska. Glob. Chang. Biol. **23**(2): 604–620. doi:10.1111/gcb.13466.

Thornton, P. K., Ericksen, P. J., Herrero, M., and Challinor, A. J. 2014. Climate variability and vulnerability to climate change: a review. Glob. Chang. Biol., **20**(11): 3313–3328. doi:10.1111/gcb.12581.

Tillotson, M.D., and Quinn, T.P. 2017. Climate and conspecific density trigger pre-spawning mortality in sockeye salmon (*Oncorhynchus nerka*). Fish. Res. **188**: 138–148. doi:10.1016/j.fishres.2016.12.013.

Trudel, M., Geist, D.R., and Welch, D.W. 2004. Modeling the oxygen consumption rates in pacific salmon and steelhead: an assessment of current models and practices. Trans. Am. Fish. Soc. **133**(2): 326–348. doi:10.1577/02-116.

Walsh, J.E., Bieniek, P.A., Brettschneider, B., Euskirchen, E.S., Lader, R., and Thoman, R.L. 2017. The exceptionally warm winter of 2015/16 in Alaska. J. Clim. **30**(6): 2069–2088. doi:10.1175/JCLI-D-16-0473.1.

Warkentin, L., Parken, C.K., Bailey, R., and Moore, J.W. 2022. Low summer river flows associated with low productivity of Chinook salmon in a watershed with shifting hydrology. Ecol. Solut. Evid. **3**(1): e12124. doi:10.1002/2688-8319.12124.

Washington State Department of Ecology. 2002. *Evaluating Criteria for the Protection of Freshwater Aquatic Life in Washington's Surface Water Quality Standards: Dissolved Oxygen*. Publication Number 00-10-071. Olympia, WA.

Wilson, K.L., Bailey, C.J., Davies, T.D., and Moore, J.W. 2022. Marine and freshwater regime changes impact a community of migratory pacific salmonids in decline. Glob. Chang. Biol. **28**(1): 72–85. doi:10.1111/gcb.15895.

Winfree, M.M., Hood, E., Stuefer, S.L., Schindler, D.E., Cline, T.J., Arp, C.D., and Pyare, S. 2018. Landcover and geomorphology influence streamwater temperature sensitivity in salmon bearing watersheds in Southeast Alaska. Environ. Res. Lett. **13**(6): 064034. doi:10.1088/1748-9326/aac4c0.

Wolman, M.G. 1954. A method of sampling coarse river-bed material. Trans. Am. Geophys. Union, **35**(6): 951–956. doi:10.1029/TR035i006p00951.

Yang, Y., Pan, M., Lin, P., Beck, H.E., Zeng, Z. Yamazaki, D., et al. 2021. Global reach-level 3-hourly river flood reanalysis (1980–2019). Bull. Am. Meteorol. Soc. **102**(11): E2086–E2105. doi:10.1175/BAMS-D-20-0057.1.

Zhang, X., Li, H.Y., Deng, Z.D., Leung, L.R., Skalski, J.R., and Cooke, S.J. 2019. On the variable effects of climate change on pacific salmon. Ecol. Model. **397**: 95–106. doi:10.1016/j.ecolmodel.2019.02.002.